had formed. The solvent was removed to yielded a red-orange solid. Further dried under high vacuum for 20 h to afford 0.550 g (79.9%) of $(C_5H_5)_2Fe_2(CO)_2(\mu\text{-}CO)(\mu\text{-}CHCH_2PPh_3)^+BF_4^-$ (19).

Preparation of $(C_5H_5)_2Fe_2(CO)_2(\mu\text{-}CO)(\mu\text{-}C{=}CH_2)$ (20). CH_3Li (2.2 mL, 1.6 M in diethyl ether) was slowly added to a solution of 6 (1.52 g, 3.45 mmol) in CH_2Cl_2 (50 mL) at -78 °C and stirred for 30 min. CH_2Cl_2 was removed, and the resulting residue was dried under high vacuum. The solid residue was taken up in benzene (70 mL) and filtered. Removal of benzene from the filtrate afforded 1.13 g (93%) of an orange-red solid of the title compound, mp 153-155 °C dec. A molecular ion (352) was observed in the mass spectrum: IR (benzene) 1995 (s), 1958 (w), 1795 (m) cm^{-1}; ^1H NMR (benzene-d_6) δ 4.25 (s, 10 H), 6.97 (s, 2 H). Anal. Calcd for $C_{15}H_{13}Fe_2O_3$: C, 51.19; H, 3.44; Fe, 31.74. Found: C, 50.97; H, 3.53; Fe, 30.98.

Reaction of $(C_5H_5)_2Fe_2(CO)_2(\mu\text{-}CO)(\mu\text{-}C{=}CH_2)$ (20) with HBF_4. A solution of aqueous HBF_4 (0.1 mL, 48%) in acetic anhydride (1.0 mL) was added to a solution of 20 (0.100 g, 0.285 mmol) in THF (40 mL) at 0 °C. The solution was warmed to room temperature and stirred for 20 min while a shining brick-red precipitate started falling out. The solid was collected and washed with THF. Application of high vacuum to remove the residual solvent afforded 0.051 g (40.8%) of complex 6.

Reaction of $(C_5H_5)_2Fe_2(CO)_2(\mu\text{-}CO)(\mu\text{-}CCH_3)^+BF_4^-$ (6) with $P(n\text{-}Bu)_3$. $P(n\text{-}Bu)_3$ (0.13 mL, 0.519 mmol) was added to a solution of 6 (0.22 g, 0.50 mmol) in acetonitrile (20 mL) at room temperature. IR spectrum of the solution indicated the formation of a new carbonyl species within 5 min. Removal of the solvent afforded a red complex of $(C_5H_5)_2Fe_2(CO)_2(\mu\text{-}CO)[\mu\text{-}CCH_3P(n\text{-}Bu)_3]^+BF_4^-$ (21) (0.26 g, 81%). Anal. Calcd for $C_{27}H_{40}BF_4Fe_2O_3P$: C, 50.50; H, 6.27; Fe, 17.39; P, 4.82. Found: C, 50.37; H, 6.05; Fe, 17.10; P, 4.64.

Acknowledgment. We wish to thank the Robert A. Welch Foundation, the National Science Foundation, and the Department of Energy for financial support.

Registry No. 1a, 81616-44-6; 1b, 81654-89-9; 2, 12154-95-9; 3, 81616-45-7; 4, 81616-46-8; 5, 81616-47-9; 6, 81616-49-1; 7, 81616-50-4; 8, 81616-52-6; 9a, 79839-80-8; 9b, 79896-43-8; 10, 25879-01-0; 11a, 75811-60-8; 11b, 75829-77-5; 14, 81616-53-7; 15, 75818-23-4; 18a, 81616-54-8; 18b, 81616-55-9; 18c, 81616-56-0; 19, 81616-58-2; 20, 76722-37-7; 21, 81616-60-6; $C_5H_5Fe(CO)(PPh_3)(CHOCH_3)^+BF_4^-$, 81616-61-7; $C_5H_5Fe(CO)_2K$, 60039-75-0.

Tridentate Amido Phosphine Derivatives of the Nickel Triad: Synthesis, Characterization, and Reactivity of Nickel(II), Palladium(II), and Platinum(II) Amide Complexes

Michael D. Fryzuk,* Patricia A. MacNeil, Steven J. Rettig, Anthony S. Secco, and James Trotter

Department of Chemistry, University of British Columbia, Vancouver, British Columbia, Canada V6T IY6

Received February 2, 1982

Deprotonation of $HN(SiMe_2CH_2PPh_2)_2$ (4) with *n*-butyllithium generates $LiN(SiMe_2CH_2PPh_2)_2$ (5), a tridentate, uninegative ligand which contains both the *hard* amido donor and *soft* phosphine donors. The reaction of 5 with each of $NiCl_2$·DME (DME = dimethoxyethane), $PdCl_2(PhCN)_2$, and $K[PtCl_3(C_2H_4)]$, generates the corresponding diamagnetic chloro amide derivatives $[MClN(SiMe_2CH_2PPh_2)_2]$ (M = Ni, 6; M = Pd, 7; M = Pt, 8). The X-ray structure of the nickel derivative 6 (space group $P\bar{1}$ (C_i^1, No. 2) a = 10.091 (3), b = 10.224 (3), c = 17.234 (4) Å; α = 81.06 (2), β = 78.51 (2), γ = 65.93 (3)°; Z = 2; R = 0.029 (R_w = 0.040)) indicates a slightly distorted square-planar geometry with trans phosphine donors. The backbone of the ring is puckered generating near C_2 symmetry in the solid state; however, the ^1H NMR is consistent with C_{2v} symmetry in solution which can be explained by a rapid conformational flipping of the ligand backbone. The X-ray structure of the corresponding palladium derivative 7 (space group $P\bar{1}$; a = 11.539 (1), b = 15.368 (2), c = 10.949 (2) Å; α = 92.92 (1), β = 104.09 (1), γ = 84.74 (1)°; Z = 2; R = 0.022 (R_w = 0.031)) also indicates trans phosphines in a square-planar array but with no puckering of the backbone of the ligand. The neutral amine 4 acts as a bidentate ligand via donation through the phosphines to produce the dichloro derivatives $[MCl_2NH(SiMe_2CH_2PPh_2)_2]$ (M = Ni, 9; M = Pd, 10; M = Pt, 11). The X-ray structure of the nickel derivative 9 (space group $P\bar{1}$; a = 10.2224 (1), b = 10.5719 (8), c = 17.770 (2) Å; α = 72.978 (6), β = 78.424 (6), γ = 61.864 (8)°; Z = 2; R = 0.031 (R_w = 0.039)) displays a distorted tetrahedral geometry with no evidence of interaction between the amine portion of the backbone and the metal. Both the palladium, 10, and platinum, 11, derivatives are assumed to be square-planar with cis disposed phosphine donors on the basis of ^1H FT NMR studies. All three dichloro derivatives, 9, 10, and 11, are cleanly converted to the corresponding chloro amide complexes, 6, 7, and 8, by treatment with NEt_3 in toluene; this reaction requires prior coordination of the phosphine donors in order to activate the distal N-H bond. Metathesis with a number of simple Grignard reagents occurs only for the nickel and palladium chloro amide derivatives, 6 and 7, to generate the metal-carbon bonded complexes $[M(R)N(SiMe_2CH_2PPh_2)_2]$ (M = Ni or Pd; R = CH_3, $CH{=}CH_2$, $CH_2CH{=}CH_2$, or C_6H_5). The platinum chloride bond of 8 does not undergo metathesis with Grignards and, in addition, is not abstracted with Ag^+; consistent with this is the Pt-Cl stretching frequency of 317 cm^{-1} which is indicative of a weak trans influence for the $^-N(SiR_3)_2$ ligand.

Introduction

The stability and reactivity of transition-metal complexes are a function of both the position of the metal in the transition series and the nature of the complexing ligands. While the former provides for a gratifying diversity of chemical behavior across the transition series, it is the latter feature which allows the reactivity patterns of a given transition metal to be fine tuned. Indeed, an enormous amount of effort has gone into the design and synthesis of new ligands[1] and new combinations of ligands[2]

(1) (a) Lukehart, C. M. *Acc. Chem. Res.* **1981**, *14*, 109. (b) King, R. B. *Ibid.* **1980**, *13*, 243. (c) Cromie, E. R.; Hunter, G.; Rankin, D. W. H. *Angew. Chem., Int. Ed. Engl.* **1980**, *19*, 316. (d) Murray, S. G.; Hartley, F. R. *Chem. Rev.* **1981**, *81*, 365. (e) Schmidbauer, H.; Deschler, U.; Milewski-Mahrla, B. *Angew. Chem., Int. Ed. Engl.* **1981**, *20*, 586.

0276-7333/82/2301-0918$01.25/0

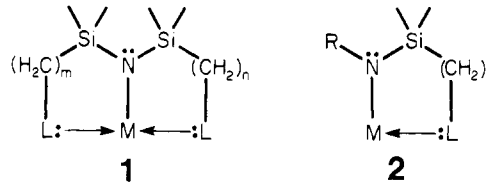

1 **2**

Figure 1. Hybrid tridentate (1) and bidentate (2) ligands (L = soft donor ligand and M = central metal atom).

which, when complexed to a transition metal, generate new and unusual chemistry.

It is useful to attempt a general classification of ligands.[3] One well-known but somewhat dated approach is according to the HSAB (hard–soft-acid–base) theory,[4] that is, classification of donor ligands as either *hard* ligands or *soft* ligands. While the boundary between these two main ligand types is sometimes indistinct, it does focus on a very important feature crucial to the HSAB theory, that of *matching* the ligand and the transition metal. For instance, the *soft* tertiary phosphine ligands, PR_3, are considered ubiquitous[5] in transition-metal complexes, yet their coordination chemistry with the "early" metals (Ti, Zr, Hf, V, Nb, Ta) is still in its infancy.[6-8] On the other hand, the *hard* amido ligand, $^-NR_2$ (R = alkyl, aryl, or silyl), forms numerous complexes with the "early" metals[9-11] but surprisingly few with low-valent group 8 metals.[12] It is this dichotomy in the coordination chemistry of these two particular ligands and related *hard–soft* pairs that has provided the impetus to design a new type of multidentate ligand, the "hybrid" ligand.[13] Our strategy involves the use of the chelate effect[16] to ensure multidenticity in "hybrid" ligands of the types shown in Figure 1, especially in cases where mismatching of *hard–soft* pairs is involved.

In this paper we describe the synthesis of a new, potentially tridentate ligand of the type 1 where L is the *soft* diphenylphosphino donor, $-PPh_2$, and its coordination chemistry with nickel(II), palladium(II), and platinum(II).[17]

Table I. ^1H NMR Data[a]

	$SiCH_3$	PCH_2	$P(C_6H_5)_2$	other
$(Ph_2PCH_2SiMe_2)_2NH$	0.1 (d, $^4J_{P,H} = 1.0$)	1.36 (d, $^2J_{P,H} \leq 1.0$)	7.18 (m), 7.58 (m)	
$LiN(SiMe_2CH_2PPh_2)_2$	−0.05 (br s)	1.58 (br s)	7.08 (m), 7.75 (m)	
$[NiClN(SiMe_2CH_2PPh_2)_2]$	0.25 (s)	1.42 (t, $J_{app} = 5.4$)	7.08 (m), 8.05 (m)	
$[NiCH_3N(SiMe_2CH_2PPh_2)_2]$	0.25 (s)	1.65 (t, $J_{app} = 6.0$)	7.05 (m), 7.78 (m)	Ni−CH_3 −0.55 (t, $J_{app} = 10.0$)
$[Ni(CH{=}CH_2)N(SiMe_2CH_2PPh_2)_2]$	0.25 (s)	1.62 (t, $J_{app} = 6.0$)	7.10 (m), 7.80 (m)	 H_1, 6.32 (m, $^3J_{1,2} = 10.8$, $^3J_{1,3} = 17.5$, $^3J_{P,1} = 6.3$), H_2, 5.18 (m, $^3J_{2,3} = 1.5$, $^4J_{P,2} = 3.5$), H_3, 4.60 (m, $^4J_{P,3} = 2.1$)
$[Ni(\eta^3\text{-}C_3H_5)N(SiMe_2CH_2PPh_2)_2]$	0.25 (br s)	1.65 (br t)	7.00 (m), 7.55 (m)	$CH(CH_2)_2$ 5.32 (quint, $J = 10.0$) $CH(CH_2)_2$ 2.32 (br d)
$[Ni(C_6H_5)N(SiMe_2CH_2PPh_2)_2]$	0.25 (s)	1.62 (t, $J_{app} = 6.0$)	7.00 (m), 7.50 (m)	NiC_6H_5 7.07 (m, 2, ortho), 6.40 (m, 3, para/meta)
$[Ni(CN)N(SiMe_2CH_2PPh_2)_2]$	0.18 (s)	1.45 (t, $J_{app} = 6.0$)	7.08 (m), 7.98 (m)	
$[PdClN(SiMe_2CH_2PPh_2)_2]$	0.25 (s)	1.52 (t, $J_{app} = 5.0$)	7.02 (m), 7.95 (m)	
$[Pd(\eta^1\text{-}C_3H_5)N(SiMe_2CH_2PPh_2)_2]$	0.15 (s)	1.78 (t, $J_{app} = 6.0$)	7.05 (m), 7.69 (m)	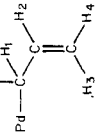 H_1, 2.24 (m, $^3J_{1,2} = 7.7$), H_2, 5.59 (m, $^3J_{2,3} = 18.0$, $^3J_{2,4} = 9.5$), H_3, 3.96 (br d), H_4, 4.31 (br d)
$[PtClN(SiMe_2CH_2PPh_2)_2]$	0.22 (s)	1.52 (tt, $J_{H,P} = 6.0$, $J_{H,Pt} = 31.0$ Hz)	7.05 (m), 7.95 (m)	

[a] All spectra were recorded in C_6D_6; chemical shifts in ppm (referenced to C_6D_6H at 7.15 ppm); coupling constants in Hz.

(2) (a) Kyba, E. P.; John, A. M.; Brown, S. B.; Hudson, C. W.; McPhaul, M. J.; Harding, A.; Larsen, K.; Niedzwiecki, S.; Davis, R. E. *J. Am. Chem. Soc.* **1980**, *102*, 139. (b) Kyba, E. P.; Chou, S.-S. P. *Ibid.* **1980**, *102*, 7012. (c) Kaufmann, T.; Ennen, J.; Lhotak, H.; Rensing, A.; Steinseifer, F.; Woltermann, A. *Angew. Chem., Int. Ed. Engl.* **1980**, *19*, 328. (d) Schore, N. E. *J. Am. Chem. Soc.* **1979**, *101*, 7410 and references therein. (e) Rauchfuss, T. B. *Ibid.* **1979**, *101*, 1045. (f) Jeffery, J. C.; Rauchfuss, T. B.; Tucker, P. A. *Inorg. Chem.* **1980**, *19*, 3306. (g) Braustein, P.; Matt, D.; Dusausoy, Y.; Fischer, J.; Mitschler, A.; Ricard, L. *J. Am. Chem. Soc.* **1981**, *103*, 5115.

(3) For a classification of ligands according to donor atom, see: Cotton, F. A.; Wilkinson, G. "Advanced Inorganic Chemistry", 4th ed., Wiley: New York, 1980; p 107.

(4) Pearson, R. G. *J. Chem. Educ.* **1968**, *45*, 581, 643.

(5) Stelzer, O. *Top. Phosphorus Chem.* **1977**, *9*, 1.

(6) (a) Datta, S.; Wreford, S. S. *Inorg. Chem.* **1977**, *16*, 1134. (b) Datta, S.; Fischer, M. B.; Wreford, S. S. *J. Organomet. Chem.* **1980**, *188*, 353. (c) Fischer, M. B.; James, E. J.; NcNeese, T. J.; Nyburg, S. C.: Posin, B.; Wong-Ng, W.; Wreford, S. S. *J. Am. Chem. Soc.* **1981**, *102*, 4941.

(7) (a) Wengrovius, J. H.; Schrock, R. R. *J. Organomet. Chem.* **1981**, *205*, 319. (b) Fellmann, J. D.; Schrock, R. R.; Rupprecht, G. A. *J. Am. Chem. Soc.* **1981**, *103*, 5752 and references therein.

(8) Schrock, R. R.; Parshall, G. W. *Chem. Rev.* **1976**, *76*, 243.

(9) Lappert, M. F.; Power, P. P.; Sanger, A. R.; Srivastava, R. C. "Metal and Metalloid Amides"; Wiley: New York, 1979.

(10) Andersen, R. A. *Inorg. Chem.* **1979**, *18*, 2928, 3622.

(11) Eller, P. G.; Bradley, D. C.; Hursthouse, M. B.; Meek, D. W. *Coord. Chem. Rev.* **1977**, *24*, 1.

(12) Cetinkaya, B.; Lappert, M. F.; Torroni, S. *J. Chem. Soc., Chem. Commun.* **1979**, 843.

(13) The term *hybrid* has been used by Sacconi[14] and others[15] to describe *neutral*, mixed-ligand systems.

(14) Bertini, I.; Dapporta, P.; Fallani, G.; Sacconi, L. *Inorg. Chem.* **1977**, *10*, 1703, and references therein.

(15) (a) Rigo, P. *Inorg. Chim. Acta* **1980**, *44*, L223. (b) MacAuliffe, C. A.; Levason, W. "Phosphine, Arsine, and Stibene Complexes of the Transition Elements"; Elsevier: Amsterdam, 1979; p 18.

(16) Reference 3, p 71.

Experimental Section

General Information. All manipulations were performed under prepurified nitrogen in a Vacuum Atmospheres HE-553-2 glovebox equipped with a MO-40-2H purifier or in standard Schlenk-type glassware. Palladium dichloride was obtained from Ventron and used as received to prepare $PdCl_2(C_6H_5CN)_2$ by a literature method.[18] Potassium tetrachloroplatinate was also obtained from Ventron and recrystallized from hot ethanol prior to use in the preparation of $K[PtCl_3(C_2H_4)]$,[19] $Pt(COD)Cl_2$,[20] $PtCl_2(C_6H_5CN)_2$,[21] *trans*-$PtCl_2(PR_3)_2$ (R = Ph[22] or Et[23]), and *trans*-$Pt(H)Cl(PEt_3)_2$.[23]

$LiPPh_2$[24] was prepared by the dropwise addition of *n*-butyllithium in hexane (1.6 M, Aldrich) to a hexane solution of $HPPh_2$. After several washings with hexane, the resultant lemon yellow powder was used directly in the preparation of $(Ph_2PCH_2SiMe_2)_2NH$.

Methylene chloride (CH_2Cl_2) and cyclohexane were purified by distillation from CaH_2 under argon. Toluene, hexanes, and diethyl ether were dried and deoxygenated from sodium benzophenone ketyl under argon. Acetone was dried by refluxing over K_2CO_3 for several days followed by distillation under argon. Tetrahydrofuran (THF) was predried by refluxing over CaH_2 and then distilled from sodium benzophenone ketyl under argon.

Melting points were determined on a Mel-Temp apparatus in sealed capillaries under nitrogen and are uncorrected. Carbon, hydrogen, and nitrogen analyses were performed by Mr. P. Borda of this department. ^1H NMR were recorded on one of the following instruments, depending upon the complexity of the particular spectrum: Varian EM-360L, Bruker WP-80, Varian XL-100, and Bruker WH-400. $^{31}P\{^1H\}$ spectra were run at 32.442 MHz on the Bruker WP-80 in 10-mm tubes fitted with inserts for the internal standard $P(OMe)_3$. C_6D_6, $(CD_3)_2CO$, C_7D_8, and $CDCl_3$ were purchased from Aldrich; the C_6D_6, $(CD_3)_2CO$, and C_7D_8 were dried over activated 4-Å molecular sieves and vacuum transferred, while the $CDCl_3$ was dried by refluxing over CaH_2 followed by vacuum transfer. Infrared spectra were recorded either on a Pye-Unicam SP-1100 or a Perkin-Elmer 598 as KBr disks or in solution.

The Grignard reagents methylmagnesium chloride (in THF) and vinyl magnesium chloride (in THF) were purchased from Ventron; phenylmagnesium bromide (in Et_2O) was obtained from Aldrich. Allylmagnesium chloride was prepared from freshly distilled allyl chloride and excess magnesium turnings in THF, filtered through cotton wool, and standardized against 0.1 M HCl.

$(Ph_2PCH_2SiMe_2)_2NH$. To a cooled solution (−4 °C) of $LiPPh_2$ (9.6 g, 0.05 mol) in THF (50 mL) was added 1,3-bis(chloromethyl)tetramethyldisilazane, $(ClCH_2SiMe_2)_2NH$[25] (5.35 g, 0.025 mol), dropwise with stirring. The initially clear red solution gradually decolorized to a very pale yellow when all of the silyl chloride had been added. The solution was stirred at room temperature for 0.5 h; the THF was then removed in vacuo. The residue was extracted with pentane (50 mL) and filtered through a medium porosity frit. Removal of the pentane in vacuo yielded a pale yellow oil which was immediately taken up in hexane (10 mL), filtered, and cooled to −4 °C. Fine white needles of the product formed; these were filtered and washed with cold hexane: yield 10.2 g (77%); mp 45–46 °C; IR (KBr disk) ν_{NH} = 3365 cm^{-1}; $^{31}P\{^1H\}$ NMR (C_6D_6) −22.45 ppm (s). Anal. Calcd for $C_{30}H_{37}NP_2Si_2$: C, 68.05; H, 6.99; N, 2.65. Found: C, 68.33; H, 7.25; N, 2.55.

$LiN(SiMe_2CH_2PPh_2)_2$. To a vigorously stirred solution of freshly recrystallized $(Ph_2PCH_2SiMe_2)_2NH$ (5.3 g, 0.01 mol) in pentane (50 mL) at room temperature was slowly added *n*-BuLi in hexane (1.6 M, 8 mL, 0.016 mol). A fine white precipitate immediately formed. After the mixture was stirred at room temperature for 0.5 h, the white solid was filtered and washed with pentane; yield 3.8 g (71%). Although the product is sufficiently pure at this stage to be used in metathetical reactions with transition-metal salts, it may be recrystallized from toluene/hexane to give colorless plates: mp 120 °C dec; $^{31}P\{^1H\}$ NMR (C_6D_6) −23.20 ppm (s). Anal. Calcd for $C_{30}H_{36}LiNP_2Si_2$: C, 67.29; H, 6.73; N, 2.61. Found: C, 67.00; H, 6.78; N, 2.48.

$[NiClN(SiMe_2CH_2PPh_2)_2]$. Method 1. A solution of $LiN(SiMe_2CH_2PPh_2)_2$ (1.34 g, 2.5 mmol) in Et_2O (25 mL) was added dropwise with stirring to a cooled (0 °C) solution of $[Ni(PMe_3)_2Cl_2]$[26] (0.7 g, 2.5 mmol) in THF (30 mL). The initially clear deep red solution immediately became dark brown in color. After being stirred at 0 °C for 0.5 h, the solution was stirred at room temperature for 1 h. The solvent was removed in vacuo and the resultant brown oil extracted with cyclohexane. Upon filtration through a medium porosity frit, a clear deep brown solution was obtained; the cyclohexane was then removed in vacuo. Recrystallization from toluene/hexane yielded diamond-shaped brown prisms: mp 153–155 °C; yield 1.01 g (65%); $^{31}P\{^1H\}$ NMR (C_6D_6) +14.76 ppm (s). Anal. Calcd for $C_{30}H_{36}ClNNiP_2Si_2$: C, 57.83; H, 5.78; N, 2.25. Found: C, 57.71; H, 5.87; N, 2.23.

Method 2. To a suspension of $NiCl_2$·DME[27] (0.22 g, 1.0 mmol) in toluene (30 mL) was added a solution of $(Ph_2PCH_2SiMe_2)_2NH$ (0.53 g, 1.0 mmol) in toluene (10 mL). Immediately, a clear deep red solution formed, and, upon stirring at room temperature for 0.5 h, green shiny needles began to precipitate. An excess of triethylamine (0.15 g, 1.5 mmol) was added dropwise, producing a deep brown solution. After being stirred at room temperature for 1 h, the solution was filtered through Celite. Removal of the solvent in vacuo yielded large brown prisms of analytically pure $[NiClN(SiMe_2CH_2PPh_2)_2]$; yield 0.55 g (88%).

$[PdClN(SiMe_2CH_2PPh_2)_2]$. A solution of $LiN(SiMe_2CH_2PPh_2)_2$ (0.54 g, 1.0 mmol) in Et_2O (10 mL) was slowly added to a cooled (−78 °C) solution of freshly prepared $(C_6H_5CN)_2PdCl_2$ (0.39 g, 1.0 mmol) in THF (30 mL); the mixture was stirred at −78 °C for 0.5 h. The clear orange-gold solution was then stirred at 0 °C for 1 h and finally at room temperature for an additional hour. The solvent was removed in vacuo and the product extracted with cyclohexane. Recrystallization from toluene/hexane gave orange blocks of the palladium amide, which contain 1 mol of toluene as solvent of crystallization: mp 136–137 °C; yield 0.40 g (60%). Anal. Calcd for $C_{37}H_{44}ClNP_2PdSi_2$: C, 58.26; H, 5.77; N, 1.83. Found: C, 58.27; H, 5.96; N, 1.81. The complex may also be recrystallized from acetone/hexane, yielding orange rod-like crystals: mp 140 °C; $^{31}P\{^1H\}$ NMR ($(CD_3)_2CO$) +18.71 ppm (s). Anal. Calcd for $C_{30}H_{36}ClNP_2PdSi_2$: C, 53.72; H, 5.37; N, 2.07. Found: C, 53.73; H, 5.54; N, 2.04.

$[PtClN(SiMe_2CH_2PPh_2)_2]$. To a cooled (0 °C) solution of freshly prepared Zeise's salt, $K[PtCl_3(C_2H_4)]$ (0.37 g, 1.0 mmol), in THF (25 mL) was slowly added a solution of $LiN(SiMe_2CH_2PPh_2)_2$ (0.54 g, 1.0 mmol) in Et_2O (10 mL). The originally clear lemon yellow solution did not undergo any noticeable color changes during the addition. The solution was stirred at 0 °C for 0.5 h and then at room temperature for 3 h. The solvent was removed in vacuo; the product was then extracted with cyclohexane, filtered, and pumped down to a fine yellow glass. Upon recrystallization from toluene/hexane, shiny yellow plates of the platinum amide were obtained: yield 0.48 g (63%); mp 147–149 °C; $^{31}P\{^1H\}$ NMR (C_6D_6) +34.27 ppm (t, $^1J_{Pt-P}$ = 2690.0 Hz). Anal. Calcd for $C_{37}H_{44}ClNP_2PtSi_2$: C, 52.23; H, 5.18; N, 1.65. Found: C, 52.10; H, 5.27; N, 1.61.

$[NiCl_2NH(SiMe_2CH_2PPh_2)_2]$. A solution of freshly recrystallized $(Ph_2PCH_2SiMe_2)_2NH$ (0.53 g, 1.0 mmol) in THF (10 mL) was added to a suspension of $NiCl_2$·DME (0.22 g, 1.0 mmol) in THF (25 mL). The solution immediately became clear deep red in color, and, upon stirring at room temperature for 0.5 h, green crystals began to form. After an additional 0.5 h, the solvent was removed in vacuo. Recrystallization of the green solid from CH_2Cl_2/hexane produced fluffy green crystals which, upon

(17) A preliminary account of a portion of this work has appeared; Fryzuk, M. D.; MacNeil, P. A. *J. Am. Chem. Soc.* **1981**, *103*, 3592.
(18) Kharasch, M. S.; Seyler, R. C.; Mayo, F. R. *J. Am. Chem. Soc.* **1938**, *60*, 882.
(19) Chock, P. B.; Halpern, J.; Paulik, F. E. *Inorg. Synth.* **1973**, *14*, 90.
(20) McDermott, J. X.; White, J. F.; Whitesides, G. M. *J. Am. Chem. Soc.* **1976**, *98*, 6521.
(21) Hartley, F. R. *Organomet. Chem. Rev., Sect. A* **1970**, *6*, 119.
(22) Hsu, C. Y.; Leshner, B. T.; Orchin, M. *Inorg. Synth.* **1979**, *19*, 114.
(23) Parshall, G. W. *Inorg. Synth.* **1970**, *12*, 26.
(24) Strecker, R. A.; Snead, J. L.; Sollott, G. P. *J. Am. Chem. Soc.* **1973**, *95*, 210.
(25) Osthoff, R. C.; Kantor, S. W. *Inorg. Synth.* **1957** *5*, 55.
(26) Dahl, O. *Acta. Chem. Scand.* **1969**, *23*, 2342.
(27) Ward, L. G. L. *Inorg. Synth.* **1972**, *13*, 154.

standing, gradually reformed as shiny blue-black prisms: yield 0.58 g (88%); mp 185–187 °C; IR (KBr disk) ν_{NH} = 3365 cm^{-1}. Anal. Calcd for $C_{30}H_{37}Cl_2NNiP_2Si_2$: C, 54.65; H, 5.66; N, 2.12. Found: C, 54.43; H, 5.67; N, 2.00.

[PdCl$_2$NH(SiMe$_2$CH$_2$PPh$_2$)$_2$]. A solution of $PdCl_2(C_6H_5CN)_2$ (0.38 g, 1.0 mmol) and $(Ph_2PCH_2SiMe_2)_2NH$ (0.53 g, 1.0 mmol) in THF (35 mL) was stirred at room temperature for 2 days. Removal of the solvent in vacuo yielded a gold-colored oil which was then recrystallized from CH_2Cl_2/cyclohexane to give yellow prisms of the product. This complex contains 1 mol of cyclohexane as solvent of crystallization: mp 140 °C; $^{31}P\{^1H\}$ NMR ($(CD_3)_2CO$) +21.86 ppm (s); IR (KBr disk) ν_{NH} = 3305 cm^{-1}. Anal. Calcd for $C_{36}H_{49}Cl_2NP_2PdSi_2$: C, 54.68; H, 6.20; N, 1.77. Found: C, 55.06; H, 6.39; N, 1.75.

[PtCl$_2$NH(SiMe$_2$CH$_2$PPh$_2$)$_2$]. Pt(COD)Cl$_2$ (0.19 g, 0.5 mmol) and $(Ph_2PCH_2SiMe_2)_2NH$ (0.27 g, 0.5 mmol) were dissolved in THF (20 mL). Upon refluxing, the milky solution gradually became clear lemon yellow in color; the solution was refluxed overnight. The solution was then cooled to room temperature, and, upon addition of hexane (30 mL), a fine white solid precipitated. The solid was filtered under nitrogen and recrystallized from CH_2Cl_2/cyclohexane to give a colorless gel which, upon standing at room temperature overnight, formed large colorless blocks: yield 0.31 g (78%); mp 220–222 °C; $^{31}P\{^1H\}$ NMR ($(CD_3)_2CO$) +41.44 ppm (t, $^1J_{Pt-P}$ = 3599.6 Hz); IR (KBr disk) ν_{NH} = 3280 cm^{-1}. Anal. Calcd for $C_{30}H_{37}Cl_2NP_2PtSi_2$: C, 45.28; H, 4.65; N, 1.76. Found: C, 45.31; H, 4.65; N, 1.69.

Conversion of Nickel(II), Palladium(II), and Platinum(II) Dichloro Amino Diphosphines to the Corresponding Chloro Amido Diphosphines. This reaction is exemplified with the palladium complex. [PdCl$_2$NH(SiMe$_2$CH$_2$PPh$_2$)$_2$·C$_6$H$_{12}$] (0.15 g, 0.2 mmol) was dissolved in toluene (15 mL) at room temperature, forming a clear gold solution. An excess of triethylamine (30 mL) was added and the solution stirred for 24 h. The resultant deep orange solution was filtered through Celite in order to remove the colorless granular NEt$_3$·HCl. Removal of the solvent in vacuo yielded the product as well-formed crystals (no further recrystallization required). In contrast with the palladium and platinum complexes, the analogous reaction to form the nickel derivative is complete within 1 h.

[Ni(CH$_3$)N(SiMe$_2$CH$_2$PPh$_2$)$_2$]. To a cooled solution (−30 °C) of [NiClN(SiMe$_2$CH$_2$PPh$_2$)$_2$] (62 mg, 0.1 mmol) in toluene (15 mL) was added CH_3MgCl in THF (2.9 M, 35 L, 0.1 mmol). The initially deep brown solution rapidly became deep orange in color. After being left standing at −30 °C for 0.5 h, the solvent was removed in vacuo. The product was extracted with hexane, filtered through Celite, and pumped down to yield fine yellow-orange crystals. Recrystallization from minimum hexane at −30 °C gave analytically pure product: mp 134–136 °C; yield 44 mg (74%); $^{31}P\{^1H\}$ NMR (C_6D_6) +26.73 ppm (s). Anal. Calcd for $C_{31}H_{39}NNiP_2Si_2$: C, 61.80; H, 6.53; N, 2.33. Found: C, 61.60; H, 6.43; N, 2.20.

[Ni(CH$_2$CH=CH$_2$)N(SiMe$_2$CH$_2$PPh$_2$)$_2$]. Allylmagnesium chloride in THF (0.55 M, 91 μL, 0.05 mmol) was added to a cooled (−30 °C) solution of [NiClN(SiMe$_2$CH$_2$PPh$_2$)$_2$] (31 mg, 0.05 mmol) in toluene (15 mL). The resultant deep red-brown solution was kept at −30 °C for 0.5 h. After being warmed to room temperature, the solvent was removed in vacuo. Extraction and recrystallization was carried out in the same manner as described for the methyl derivative, yielding deep red-brown crystals: mp 130 °C dec; yield 24 mg (78%); $^{31}P\{^1H\}$ NMR (C_6D_6) +17.81 ppm (br s). Anal. Calcd for $C_{33}H_{41}NNiP_2Si_2$: C, 63.06; H, 6.53; N, 2.23. Found: C, 62.82; H, 6.80; N, 2.13.

[Ni(CH=CH$_2$)N(SiMe$_2$CH$_2$PPh$_2$)$_2$]. Addition of vinylmagnesium bromide in THF (1.4 M, 72 μL, 0.1 mmol) to a cooled (−30 °C) solution of [NiClN(SiMe$_2$CH$_2$PPh$_2$)$_2$] (62 mg, 0.1 mmol) in toluene (60 mL) produced a gold-brown solution. After 20 min at −30 °C, the solvent was removed in vacuo. Extraction with hexane, followed by filtration through Celite and solvent removal, yielded gold crystals of the vinyl derivative: mp 215–220 °C dec; yield 40 mg (65%). Anal. Calcd for $C_{32}H_{39}NNiP_2Si_2$: C, 62.54; H, 6.35; N, 2.28. Found: C, 62.48; H, 6.44; N, 2.11.

[Ni(C$_6$H$_5$)N(SiMe$_2$CH$_2$PPh$_2$)$_2$]. To a cooled solution (−30 °C) of [NiClN(SiMe$_2$CH$_2$PPh$_2$)$_2$] (62 mg, 0.1 mmol) in THF (60 mL) was added phenylmagnesium bromide in Et$_2$O (3.0 M, 34 μL, 0.1 mmol). After 15 min at −30 °C, the solvent was removed in vacuo. Extraction with hexane gave gold-brown crystals of the phenyl derivative: mp 160–162 °C dec; yield 40 mg (60%). Anal. Calcd for $C_{36}H_{41}NNiP_2Si_2$: C, 65.06; H, 6.35; N, 2.28. Found: C, 65.58; H, 6.35, N, 2.06.

[Ni(CN)N(SiMe$_2$CH$_2$PPh$_2$)$_2$]. Freshly distilled Me_3SiCN (44 mg, 0.45 mmol) was added at room temperature to a solution of NiClN(SiMe$_2$CH$_2$PPh$_2$)$_2$ (0.25 g, 0.4 mmol) in toluene (25 mL). After stirring at room temperature for 45 min, the reaction mixture rapidly changed from its initial deep brown color to a clear orange. The solution was stirred at room temperature for an additional 2 h, after which time the solvent was removed in vacuo. Recrystallization of the resultant orange oil from toluene/hexane yielded small orange blocks of the cyanide complex: mp 142–143 °C; yield 20 mg (83%); IR (KBr disk) ν_{CN} = 2122 cm^{-1}. Anal. Calcd for $C_{31}H_{36}N_2NiP_2Si_2$: C, 60.68; H, 5.87; N, 4.56. Found: C, 61.00; H, 6.00; N, 4.40.

[Pd(CH$_3$)N(SiMe$_2$CH$_2$PPh$_2$)$_2$]. The synthesis of this complex was performed in a fashion identical with that as outlined for the nickel analogue. Upon addition of the Grignard, the starting gold-colored solution became completely colorless. Recrystallization of the product from minimum hexane at −30 °C yielded colorless plates: mp 134–136 °C; yield 48 mg (74%); $^{31}P\{^1H\}$ NMR (C_6D_6) +24.92 ppm (s). Anal. Calcd for $C_{31}H_{39}NP_2PdSi_2$: C, 57.28; H, 6.05; N, 2.15. Found: C, 57.17; H, 6.10; N, 1.82.

[Pd(CH$_2$CH=CH$_2$)N(SiMe$_2$CH$_2$PPh$_2$)$_2$]. Preparation of this complex followed that of the corresponding nickel derivative. The product was obtained as pale yellow crystals from hexane: mp 90 °C dec; yield 29 mg (86%). Anal. Calcd for $C_{33}H_{41}NP_2PdSi_2$: C, 58.67; H, 6.07; N, 2.07. Found: C, 59.23; H, 6.42; N, 2.13.

X-ray Crystallographic Analyses of [NiClN(SiMe$_2$CH$_2$PPh$_2$)$_2$], 6, [PdClN(SiMe$_2$CH$_2$PPh$_2$)$_2$]·CH$_3$C$_6$H$_5$, 7, and [NiCl$_2$NH(SiMe$_2$CH$_2$PPh$_2$)$_2$], 9. Crystallographic data for **6**, **7**, and **9** are given in Table II. Crystals were mounted on an Enraf-Nonius CAD4-F diffractometer in nonspecific orientations. Final unit-cell parameters were obtained by least-squares on (2 sin θ)/λ values for 25 reflections (with $20 \le 2\theta \le 50°$ for **6** and **7** and $36 \le 2\theta \le 45°$ for **9**) measured with Mo K α_1 radiation (λ = 0.709 30 Å).

The intensities of three check reflections were measured every hour throughout the data collections and in each case showed only random fluctuations. Totals of 7236, 8509, and 7370 independent data with $2\theta \le 55°$ were measured and processed[28] for **6**, **7**, and **9**, respectively. Of these, 5124, 6081, and 4629 had $I \ge 3\sigma(I)$ and were used in the solution and refinement of the structures. Absorption corrections were applied by using the Gaussian integration method;[29,30] transmission factor ranges are given in Table II.

The centrosymmetric space group $P\bar{1}$ was chosen in each case on the basis of the E statistics and the Patterson functions. All three structures were solved by conventional heavy-atom techniques; all atoms (including hydrogen) not located from the Patterson function were positioned from successive difference Fourier maps. In the final cycles of full-matrix least-squares refinement all nonhydrogen atoms were refined with anisotropic thermal parameters and hydrogen atoms with isotropic thermal parameters. Neutral atom scattering factors from ref 31 were used for the nonhydrogen atoms and those of ref 32 for hydrogen atoms. Anomalous scattering factors from ref 33 were used for Pd, Ni, Cl, P, and Si atoms.

Mean and maximum parameter shifts on the final cycles of refinement corresponded to 0.03 and 0.19σ for **6**, 0.03 and 0.38σ for **7**, and 0.08 and 1.0σ for **9**. Final difference maps for all three

(28) The computer programs used include locally written programs for data processing and locally modified versions of the following: AGNOST, absorption correction from Northwestern University; ORFLS, full-matrix least squares, and ORFFE, function and errors, by W. R. Busing, K. O. Martin, and H. A. Levy; FORDAP, Patterson and Fourier synthesis, by A. Zalkin; ORTEP II, illustrations, by C. K. Johnson.

(29) Coppens, P.; Leiserowitz, L.; Rabinovich, D. *Acta Crystallogr.* **1965**, *18*, 1035.

(30) Busing, W. R., Levy, H. A. *Acta. Crystallogr.* **1967**, *22*, 457.

(31) Cromer, D. T.; Mann, J. B. *Acta Crystallogr., Sect. A* **1968**, *A24*, 321.

(32) Stewart, R. F.; Davidson, E. R.; Simpson, W. T. *J. Chem. Phys.* **1965**, *42*, 3175.

(33) Cromer, D. T.; Liberman, D. *J. Chem. Phys.* **1970**, *53*, 1891.

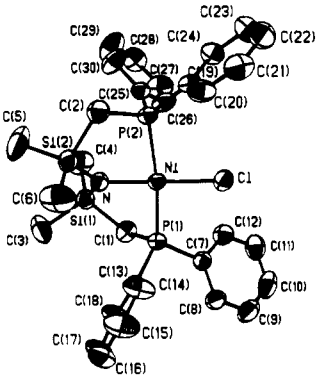

Figure 2. Labeling scheme for the atoms of $[NiClN(SiMe_2CH_2PPh_2)_2]$ (**6**). Ellipsoids are shown for the 50% probability level.

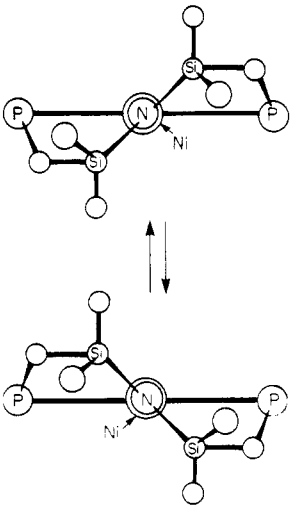

Figure 3. Proposed rotation of the NSi_2 part of the backbone for the exchange of the backbone substituents.

structures showed no unusual features; the largest fluctuations (all near heavy atoms) were 0.30, 0.31, and 0.60 e Å^{-3} for **6**, **7**, and **9**, respectively. Final positional and isotropic [or equivalent isotropic, U_{eq} = 1/3 trace (U_{diag})] thermal parameters for **6**, **7**, and **9** are given in Tables III, IV, and V, respectively. Anisotropic thermal parameters (Tables VI–VIII) and measured and calculated structure factors (Tables IX–XI) for the three structures are included as supplementary material.

The thermal motion in all three structures has been analyzed in terms of the rigid-body modes of translation, libration, and screw motion.[34] The root-mean-square errors in the temperature factors, σU_{ij} (derived from the least-squares analyses), are 0.0015, 0.0019, and 0.0016 Å^2 for **6**, **7**, and **9**, respectively. Those groups for which ΔU_{ij} is less than three times σU_{ij} have been regarded as rigid bodies. In each case analysis of all nonhydrogen atoms indicated significant independent motion of the PPh groups and in the case of **9** indicated the $SiMe_2$ moieties. Smaller segments of the molecules were then analyzed and appropriate distances have been corrected for libration[35] by using shape parameters q^2 of 0.08 for all atoms involved. Corrected bond lengths for the three compounds appear along with the uncorrected values in Tables XII–XIV and corrected bond angles are essentially equal to the uncorrected values listed in Tables XV–XVII. Intraannular torsion angles defining the conformations of nonplanar rings appear in Table XVIII. Bond lengths and angles involving hydrogen atoms and complete listings of torsion angles for all three compounds (Tables XIX–XXVII) are included as supplementary material. Atom labeling for **6**, **7**, and **9** is shown in Figures 2, 4, and 5, respectively.

(34) Schomaker, V.; Trueblood, K. N. *Acta Crystallogr., Sect. B* **1968**, *A24*, 63.
(35) Cruickshank, D. W. J. *Acta Crystallogr.* **1956**, *9*, 747; **1956**, *9*, 754; **1961**, *14*, 896.

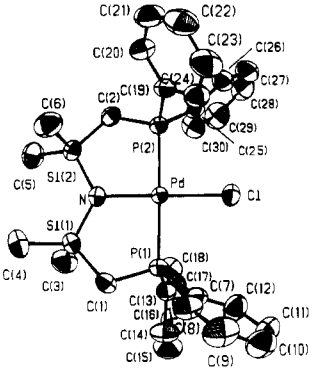

Figure 4. Labeling scheme for the atoms of $[PdClN(SiMe_2CH_2PPh_2)_2]$ (**7**). Ellipsoids are shown for the 50% probability level.

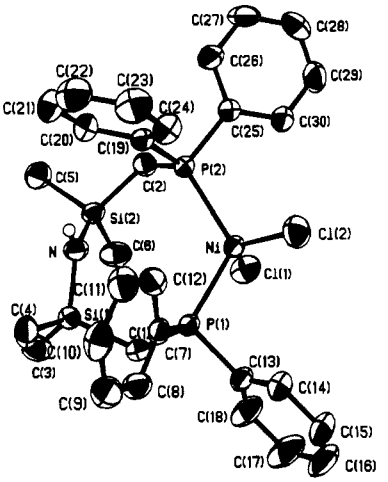

Figure 5. Labeling scheme for the atoms of $[NiCl_2NH(SiMe_2CH_2PPh_2)_2]$ (**9**). Ellipsoids are shown for the 50% probability level.

Results

Ligand Synthesis. The reaction of 2 equiv of $LiPPh_2$ with 1,3-bis(chloromethyl)tetramethyldisilazane,[25] $(ClCH_2SiMe_2)_2NH$ (**3**), in tetrahydrofuran (THF) produces the new hybrid tridentate ligand 1,3-bis((diphenylphosphino)methyl)tetramethyldisilazane, $(Ph_2PCH_2SiMe_2)_2NH$ (**4**), in good yields. We normally synthesize **4** in 10-g batches; however, three- or fourfold scaleups do not affect the yield. The ligand is easily obtained as colorless, moisture-sensitive crystals by recrystallization from cold (−30 °C) hexane. Although **4** can be used directly as a

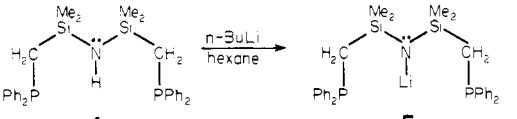

4 **5**

chelating ligand (vide infra), it can also be deprotonated with *n*-butyllithium (*n*-BuLi) to generate the crystalline lithio derivative **5**; this is a convenient reagent for metathetical reactions with a variety of suitable transition-metal halides, in analogy to other work with monodentate amido precursors.[9,10,12,36]

Coordination Chemistry. The reaction of **5** with soluble nickel(II) complexes of the type $NiCl_2(PR_3)_2$ (R = Ph[37] or Me[26]) in THF at 0 °C produces the deep orange-brown crystalline, *diamagnetic* nickel(II) derivative,

(36) Simpson, S. J.; Turner, H. W.; Andersen, R. A. *J. Am. Chem. Soc.* **1979**, *101*, 7728, and references therein.
(37) Venanzi, L. M. *J. Chem. Soc.* **1958**, 719.

Table II. Crystallographic Data[a]

	$[NiClN(SiMe_2CH_2PPh_2)_2]$, 6	$[PdClN(SiMe_2CH_2PPh_2)_2]\cdot CH_3C_6H_5$, 7	$[NiCl_2NH(SiMe_2CH_2PPh_2)_2]$, 9
formula	$C_{30}H_{36}ClNNiP_2Si_2$	$C_{37}H_{44}ClNP_2PdSi_2$	$C_{30}H_{37}Cl_2NNiP_2Si_2$
fw	622.9	762.75	659.37
cryst system	triclinic	triclinic	triclinic
a, Å	10.091 (3)	11.539 (1)	10.2224 (7)
b, Å	10.224 (3)	15.368 (2)	10.5719 (8)
c, Å	17.237 (4)	10.949 (2)	17.770 (2)
α, deg	81.06 (2)	92.92 (1)	72.978 (6)
β, deg	78.51 (2)	104.09 (1)	78.424 (6)
γ, deg	65.93 (3)	84.74 (1)	61.864 (8)
cell vol, Å^3	1585.7 (9)	1874.5 (5)	1615.6 (2)
Z	2	2	2
D_{calcd}, g cm^{-3}	1.304	1.351	1.356
space group	$P\bar{1}$ (C_i^1, No. 2)	$P\bar{1}$	$P\bar{1}$
$F(000)$	652	788	674
cryst dimens, mm	0.23 × 0.33 × 0.60	0.21 × 0.21 × 0.25	0.24 × 0.25 × 0.28
μ (Mo Kα), cm^{-1}	8.92	7.32	9.59
transmission factors	0.766-0.837	0.803-0.893	0.797-0.829
scan type	ω-$^5/_3\theta$	ω-$^4/_3\theta$	ω-2θ
ω scan speed, deg min^{-1}	1.18-10.06	1.26-10.06	1.34-10.06
scan range, deg in ω	0.60 + 0.35 tan θ	0.60 + 0.35 tan θ	0.90 + 0.35 tan θ
data collected	$\pm h,\pm k,+l$	$\pm h,\pm k,+l$	$+h,\pm k,\pm l$
2θ(max), deg	55	55	55
unique reflctns	7236	8509	7370
obsd reflctns	5124	6081	4629
no. of variables	478	573	491
R (obsd reflctns)	0.029	0.022	0.031
R_w (obsd reflctns)	0.040	0.031	0.039
R (all data)	0.054	0.051	0.071
error in observn of unit weight	1.499	1.091	1.564

[a] The following data apply to all three structure analyses: temperature 21 ± 1 °C; Mo Kα radiation, graphite monochometer, λ = 0.710 73 Å; take off angle 2.7°; lattice constants refer to reduced cell; aperature (2.0 + tan θ) × 4.0 mm at a distance of 173 mm from crystal; scan range extended by 25% on both sides for background measurement; $\sigma^2(I) = S + 2B + [0.04(S - B)]^2$ (S = scan count, B = background count); function minimized $\Sigma w(|F_o| - |F_c|)^2$, where $w = 1/\sigma^2(F)$, $R = \Sigma ||F_o| - |F_c||/\Sigma |F_o|$, and $R_w = (\Sigma w(|F_o| - |F_c|)^2/\Sigma w|F_o|^2)^{1/2}$.

$[NiClN(SiMe_2CH_2PPh_2)_2]$ (6). The use of anhydrous $NiCl_2$ or $NiBr_2$ has produced impure mixtures of compounds presumably due to the starting material's relative insolubility. Indeed, the best source of nickel(II) that we have found is $NiCl_2$·DME[27] (DME = 1,2-dimethoxyethane); it has sufficient solubility to give high yields of pure 6 and also avoids the sometimes tedious separation from nonvolatile phosphine side products as is the case when the starting nickel complex is $NiCl_2(PPh_3)_2$. That a diamagnetic nickel(II) derivative is formed in all these reactions contrasts earlier work[38] in which the paramagnetic nickel(I) complex $[NiN(SiMe_3)_2(PPh_3)_2]$ was obtained from the analogous reaction of $LiN(SiMe_3)_2$ and $NiCl_2(PPh_3)_2$.

Diagnostic of a trans orientation of the chelated phosphine donors in 6 is the presence of a virtual triplet[39] for the methylene resonance (PCH_2Si) of the ligand in the ^1H NMR (Table I). The same trans configuration also exists in the solid state as determined by single crystal X-ray analysis (Figure 2). 6 adopts a distorted square-planar geometry as indicated by the bond angles around the nickel center (Table XV); both P–Ni–Cl angles of 93.74 (2)° and 95.40 (2)° are greater than the expected 90° angles. the Ni–N bond distance (Table XII) of 1.924 (2) Å in 6 is longer than that found in the nickel(I) derivative $[NiN(SiMe_3)_2(PPh_3)_2]$ (Ni–N = 1.870 (8) Å; however, the Ni–P bond lengths in 6, 2.1975 (5) and 2.2086 (6) Å, are nearly identical with those found in the same Ni(I) derivative.[38]

Of particular interest is the observed puckering of the backbone of the chelate ring in the solid state. The planar $ClNiNSi_2$ portion of the molecule is tilted by approximately 40° with respect to the coordination plane of the nickel complex, resulting in a Si(1) deviation of +0.89 Å and a Si(2) deviation of −1.25 Å away from the least-squares plane through the complex. This puckering is further reflected in the geometry about the nitrogen: the Si–N–Si bond angle of 128.13 (10)° is larger than the expected[11] value of 120°. In addition, the methyl groups on one silicon atom are staggered with respect to those on the other silicon atom, thereby minimizing their interaction energy. The closest intramolecular approach between methyls on different silicon atoms is 3.629 (7) Å which is only slightly greater than the calculated[40] van der Waals distance, $2\bar{r}_w(CH_3)$ = 3.56 Å.

The two phenyl groups on each phosphorus atom are arranged such that the ring planes are roughly perpendicular to each other. The Ni–P(1)–C(7) and Ni–P(2)–C(19) angles show noticeable increases over tetrahedral values owing in part to the bulkiness of the phenyl substituents. Contacts of 3.400 (2) and 3.366 (2) Å occur between Cl and atoms C(7) and C(19), respectively.

Deviations of less than 5° are observed in the Si–C–P angles, indicating minimal angular strain at these vertices. Other bond lengths and angles generally agree with accepted values.[11]

In principle, the near C_2 symmetry displayed in the solid state should lead to nonequivalent substituents along the ligand backbone; for example, the silyl methyls adopt axial and equatorial dispositions which, if the chelate rings are fixed, should be diastereotopic in solution. However, at ambient temperatures, these silyl methyls are equivalent

(38) Bradley, D. C.; Hursthouse, M. B. Smallwood, R. J.; Welch, A. J. *J. Chem. Soc., Chem. Commun.* **1972**, 872.
(39) Brookes, P. R.; Shaw, B. L. *J. Chem. Soc. A* **1967**, 1079.
(40) Edward, J. J. *J. Chem. Educ.* **1970**, *47*, 261.

Table III. Final Positional (Fractional, $\times 10^5$; H, $\times 10^3$) and Isotropic Thermal Parameters ($U \times 10^3$ Å^2) with Estimated Standard Deviations in Parentheses for $[NiClN(SiMe_2CH_2PPh_2)_2]$, 6

atom	x	y	z	U_{eq}/U_{iso}
Ni	18682 (3)	31224 (2)	27070 (1)	34
Cl	−567 (6)	50909 (6)	29100 (3)	49
P(1)	28839 (6)	40112 (6)	16176 (3)	36
P(2)	10107 (6)	18336 (6)	36472 (3)	37
Si(1)	42497 (6)	8497 (6)	16203 (4)	43
Si(2)	42152 (7)	4948 (7)	34296 (4)	47
N	35788 (19)	13681 (18)	25628 (11)	40
C(1)	34598 (29)	25728 (25)	9639 (14)	48
C(2)	25126 (27)	6831 (29)	41757 (15)	52
C(3)	62850 (34)	826 (55)	13881 (27)	81
C(4)	35940 (48)	−4517 (40)	13391 (25)	75
C(5)	53717 (61)	−14484 (43)	33621 (30)	110
C(6)	52436 (64)	13450 (66)	38158 (30)	98
C(7)	17629 (23)	56159 (22)	10559 (12)	41
C(8)	21417 (30)	67792 (25)	7841 (15)	51
C(9)	12535 (36)	79255 (28)	3309 (18)	68
C(10)	−202 (36)	79269 (30)	1667 (17)	70
C(11)	−4283 (31)	68045 (31)	4496 (17)	63
C(12)	4571 (26)	56407 (27)	8965 (14)	51
C(13)	44541 (22)	43697 (23)	17320 (12)	40
C(14)	44787 (32)	48068 (34)	24397 (15)	64
C(15)	56425 (38)	51139 (41)	25418 (19)	78
C(16)	67691 (31)	50119 (33)	19446 (19)	67
C(17)	67609 (30)	45928 (37)	12365 (20)	73
C(18)	56172 (29)	42532 (34)	11304 (17)	64
C(19)	−5920 (23)	26814 (22)	43716 (12)	40
C(20)	−4894 (31)	34755 (29)	49252 (15)	56
C(21)	−17006 (34)	42037 (30)	54523 (16)	63
C(22)	−30303 (33)	41468 (31)	54322 (16)	65
C(23)	−31461 (30)	33544 (32)	48970 (17)	63
C(24)	−19341 (25)	26288 (27)	43609 (14)	50
C(25)	4864 (21)	7171 (21)	31515 (12)	38
C(26)	−2081 (31)	13219 (31)	24984 (16)	56
C(27)	−6506 (33)	5395 (35)	20960 (17)	67
C(28)	−3820 (32)	−8668 (33)	23463 (19)	67
C(29)	2996 (42)	−14800 (32)	29876 (24)	83
C(30)	7318 (35)	−7020 (28)	34035 (19)	66
H1(1)	414 (3)	268 (3)	51 (2)	72 (9)
H2(1)	263 (3)	262 (3)	77 (1)	57 (7)
H1(2)	256 (3)	114 (3)	464 (2)	78 (9)
H2(2)	251 (3)	−22 (3)	440 (2)	84 (10)
H1(3)	665 (4)	−74 (4)	157 (2)	98 (14)
H2(3)	661 (4)	2 (4)	88 (2)	104 (13)
H3(3)	664 (5)	44 (5)	169 (3)	125 (17)
H1(4)	259 (6)	−15 (5)	146 (3)	147 (19)
H2(4)	388 (4)	−130 (5)	170 (3)	120 (15)
H3(4)	404 (4)	−62 (4)	87 (2)	96 (12)
H1(5)	449 (5)	203 (5)	400 (3)	143 (24)
H2(5)	548 (4)	100 (4)	431 (2)	97 (11)
H3(5)	586 (5)	154 (5)	346 (3)	117 (16)
H1(6)	555 (5)	−196 (5)	386 (3)	136 (16)
H2(6)	625 (5)	−152 (5)	307 (3)	129 (18)
H3(6)	521 (6)	−214 (6)	300 (3)	178 (22)
H(8)	292 (3)	674 (3)	90 (2)	53 (7)
H(9)	155 (3)	877 (3)	21 (2)	77 (9)
H(10)	−55 (3)	869 (3)	−16 (2)	76 (9)
H(11)	−132 (3)	683 (3)	33 (2)	74 (9)
H(12)	22 (3)	475 (3)	108 (2)	60 (7)
H(14)	370 (3)	487 (3)	287 (2)	80 (9)
H(15)	564 (4)	531 (4)	300 (2)	100 (12)
H(16)	760 (3)	517 (3)	201 (2)	77 (9)
H(17)	762 (3)	450 (3)	81 (2)	93 (10)
H(18)	551 (3)	403 (3)	62 (2)	91 (10)
H(20)	48 (3)	347 (3)	495 (2)	80 (9)
H(21)	−161 (4)	465 (4)	586 (2)	99 (11)
H(22)	−386 (4)	479 (4)	578 (2)	97 (11)
H(23)	−406 (4)	336 (4)	490 (2)	96 (11)
H(24)	−206 (3)	206 (3)	396 (1)	56 (7)
H(26)	−41 (4)	217 (4)	233 (2)	90 (11)
H(27)	−110 (3)	99 (3)	165 (2)	74 (9)
H(28)	−63 (4)	−140 (4)	208 (2)	100 (11)
H(29)	40 (4)	−238 (4)	318 (2)	112 (13)
H(30)	114 (4)	−108 (4)	385 (2)	93 (11)

and appear as a sharp singlet in the ^{1}H NMR (Table I) indicative of C_{2v} rather than C_2 symmetry; furthermore the methylene resonances do not exhibit the complexity expected for a locked, puckered conformation; rather, a virtual triplet is observed, indicating either rapid conformational flipping of the puckered backbone or accidental equivalence. At −80 °C, the ^{1}H NMR spectrum shows broadened resonances and, interestingly, a *decrease* in peak intensity (by 50 ± 5%) as measured by integration vs. the residual protons solvent peak ($(CD_3)_2CO$ or $C_6D_5CD_3$). In addition, at −80 °C, the originally deep brown solution turns *bright green* and remains clear of solids. We originally suggested that the paramagnetic tetrahedral isomer of $[NiClN(SiMe_2CH_2PPh_2)_2]$ was being stabilized at low temperature; however, we have been unable to provide further support for this hypothesis. Low-temperature visible and near-infrared spectroscopy proved insensitive to this color change, and no absorptions normally characteristic of d^8 tetrahedral complexes were observed. Attempts to detect paramagnetism at low temperature by Evan's method[41] indicated only diamagnetic species within the detectability of the experiment. If an energetically accessible tetrahedral isomer is necessary to effect conformational flipping of the backbone, then on the basis of simple ligand field theory, a strong field ligand such as cyanide should stabilize the square-planar isomer and lock a puckered conformation of the ligand. The reaction of Me_3SiCN[42] with **6** easily generates the cyanide derivative $[Ni(CN)N(SiMe_2CH_2PPh_2)_2]$, which exhibits ^{1}H NMR (Table I) consistent with rapid conformational flipping of the backbone at all temperatures exactly analogous to **6**. Based on this result, it is unnecessary to invoke any isomerization to the tetrahedral isomer; furthermore the conformational flipping of the backbone can be rationalized as a simple rotation of the planar NSi_2 fragment through the square plane of the complex as shown in Figure 3.

The reaction of the lithium salt **5** with $PdCl_2(PhCN)_2$ in THF at −80 °C produces the analogous palladium(II) derivative $[PdClN(SiMe_2CH_2PPh_2)_2]$, **7**, as an orange crystalline solid; to our knowledge, this is the *first* stable palladium amide complex. The metathesis reaction to form **7** is surprisingly temperature dependent; if the reaction of **5** with $PdCl_2(PhCN)_2$ is carried out at ambient temperatures, much insoluble residue forms and the yield of **7** is drastically reduced. Once again the presence of a "virtual" triplet in the ^{1}H NMR (Table I) indicates a trans structure in solution. This has been verified for the solid state as well as by X-ray analysis; the structure is shown in Figure 4. Notable in this structure is the absence of gross puckering in the backbone of the chelate rings. Whereas in both the nickel(II) derivative **6** and in the nickel(I) complex $[NiN(SiMe_3)_2(PPh_3)_2]$, the planar NSi_2 framework is tilted with respect to the coordination plane, the palladium derivative **7** has the NSi_2 fragment virtually coplanar with the least-squares plane of the complex. This is due to the longer Pd–P (2.3078 (5), 2.3112 (5) Å) and Pd–N (2.063 (2) Å) bonds compared to Ni–P (2.2086 (6), 2.1975 (5) Å) and Ni–N (1.924 (2) Å) bonds, all of which allow the backbone of the ligand to expand and generate nearly eclipsed silyl methyl groups; the closest approach between methyls on different silicon atoms of **7** is 3.738 (6) Å. The overall result of the expanded chelate rings is a flattened ligand system and a complex with near C_{2v} symmetry. It is further noted that the angles around nitrogen are closer to 120° in **7** than in **6**, suggesting less

(41) Evans, D. F. *J. Chem. Soc.* **1958**, 2003.
(42) Andersen, R. A. *Inorg. Nucl. Chem. Lett.* **1980**, *16*, 31.

Table IV. Final Positional (Fractional, $\times 10^5$; H, $\times 10^3$) and Isotropic Thermal Parameters ($U \times 10^3$ Å^2) with Estimated Standard Deviations in Parentheses for $[PdClN(SiMe_2CH_2PPh_2)_2]\cdot CH_3C_6H_5$, 7

atom	x	y	z	U_{eq}/U_{iso}	atom	x	y	z	U_{eq}/U_{iso}
Pd	22723 (1)	20955 (1)	18865 (1)	32	H1(1)	35 (3)	404 (2)	201 (3)	65 (8)
P(1)	14246 (5)	32902 (3)	6940 (5)	37	H2(1)	105 (2)	472 (2)	141 (2)	40 (6)
P(2)	32064 (5)	9366 (3)	31200 (5)	38	H1(2)	489 (3)	153 (2)	429 (3)	58 (8)
Cl	18053 (6)	11778 (4)	1248 (5)	52	H2(2)	440 (2)	105 (2)	513 (3)	58 (8)
Si(1)	23817 (6)	40334 (4)	32561 (6)	48	H1(3)	423 (4)	461 (3)	374 (4)	114 (16)
Si(2)	33571 (6)	24885 (4)	48687 (6)	45	H2(3)	344 (3)	514 (3)	289 (3)	94 (12)
N	26937 (17)	29295 (11)	34386 (17)	43	H3(3)	414 (4)	434 (3)	251 (4)	111 (15)
C(1)	11400 (23)	41598 (15)	17813 (24)	48	H1(4)	99 (5)	425 (3)	471 (5)	149 (19)
C(2)	41517 (23)	14150 (17)	45074 (23)	48	H2(4)	237 (4)	464 (3)	531 (5)	132 (17)
C(3)	36901 (36)	46090 (24)	30765 (43)	74	H3(4)	150 (4)	504 (3)	430 (4)	93 (14)
C(4)	17807 (47)	46016 (26)	45526 (40)	84	H1(5)	433 (4)	363 (3)	604 (4)	97 (14)
C(5)	45479 (40)	31544 (28)	58422 (36)	77	H2(5)	512 (4)	321 (3)	536 (4)	118 (16)
C(6)	22741 (36)	23012 (27)	58138 (35)	73	H3(5)	487 (4)	294 (3)	660 (4)	125 (16)
C(7)	681 (20)	32063 (14)	−5565 (22)	44	H1(6)	156 (4)	201 (3)	531 (4)	110 (14)
C(8)	−10479 (24)	33745 (20)	−3186 (31)	61	H2(6)	254 (4)	196 (3)	642 (4)	112 (14)
C(9)	−20671 (30)	32954 (26)	−12863 (42)	84	H3(6)	188 (4)	285 (3)	600 (4)	110 (14)
C(10)	−19828 (36)	30454 (25)	−24588 (42)	90	H(8)	−111 (2)	356 (2)	43 (3)	51 (8)
C(11)	−8871 (38)	28661 (26)	−27124 (34)	89	H(9)	−281 (4)	339 (3)	−108 (4)	126 (16)
C(12)	1363 (30)	29433 (22)	−17535 (29)	70	H(10)	−273 (4)	300 (3)	−304 (4)	134 (16)
C(13)	24671 (21)	37043 (14)	−976 (21)	44	H(11)	−86 (3)	267 (2)	−358 (4)	95 (11)
C(14)	21378 (31)	44425 (20)	−8219 (32)	72	H(12)	78 (3)	284 (2)	−189 (3)	61 (9)
C(15)	29579 (42)	47840 (25)	−13620 (37)	87	H(14)	133 (3)	469 (2)	−95 (3)	97 (12)
C(16)	40850 (38)	43948 (24)	−12045 (35)	82	H(15)	271 (3)	522 (2)	−176 (4)	95 (12)
C(17)	44103 (32)	36654 (22)	−5091 (36)	75	H(16)	460 (3)	461 (2)	−157 (3)	98 (12)
C(18)	36077 (24)	33143 (17)	393 (27)	56	H(17)	519 (3)	347 (2)	−37 (3)	94 (12)
C(19)	22075 (21)	2645 (14)	36299 (22)	45	H(18)	390 (3)	280 (2)	59 (3)	63 (8)
C(20)	24990 (29)	−774 (19)	48302 (27)	61	H(20)	321 (3)	7 (2)	541 (3)	60 (8)
C(21)	17356 (38)	−6258 (22)	51550 (36)	79	H(21)	196 (3)	−84 (2)	594 (4)	101 (12)
C(22)	7236 (38)	−8376 (23)	43130 (41)	84	H(22)	18 (3)	−118 (2)	452 (3)	84 (10)
C(23)	4448 (34)	−5164 (23)	31199 (41)	82	H(23)	−14 (4)	−61 (3)	249 (4)	117 (16)
C(24)	11797 (25)	418 (18)	27806 (28)	60	H(24)	98 (2)	29 (2)	193 (3)	59 (8)
C(25)	41626 (20)	1512 (14)	24301 (20)	43	H(26)	326 (3)	−88 (2)	241 (3)	68 (9)
C(26)	39660 (28)	−7227 (17)	22328 (27)	58	H(27)	456 (3)	−185 (2)	163 (3)	78 (10)
C(27)	47323 (33)	−12842 (20)	17058 (31)	73	H(28)	618 (3)	−141 (2)	99 (3)	103 (12)
C(28)	56942 (31)	−9920 (23)	13862 (29)	72	H(29)	651 (4)	9 (2)	133 (4)	103 (13)
C(29)	58908 (33)	−1296 (26)	15631 (34)	79	H(30)	524 (3)	99 (2)	215 (3)	81 (10)
C(30)	51287 (29)	4417 (21)	20825 (32)	67	H(32)	15 (4)	−216 (3)	−266 (4)	113 (16)
C(31)	18244 (31)	−19472 (22)	−17085 (34)	77	H(33)	77 (4)	−315 (3)	−417 (4)	118 (15)
C(32)	9341 (43)	−23130 (35)	−26397 (47)	99	H(34)	276 (4)	−351 (3)	−400 (4)	124 (18)
C(33)	12379 (62)	−28886 (39)	−35165 (50)	117	H(35)	400 (4)	−303 (3)	−271 (4)	119 (17)
C(34)	24253 (72)	−31218 (33)	−35101 (51)	117	H(36)	345 (3)	−198 (2)	−106 (4)	93 (13)
C(35)	32914 (52)	−27699 (30)	−26101 (45)	100	H1(37)	72 (6)	−141 (4)	−56 (6)	178 (24)
C(36)	29892 (33)	−21923 (23)	−17271 (38)	77	H2(37)	141 (6)	−75 (5)	−98 (6)	195 (29)
C(37)	15022 (52)	−13286 (35)	−7252 (66)	107	H3(37)	205 (8)	−127 (5)	16 (8)	279 (45)

angular strain at nitrogen in the former structure. The geometry around palladium is very close to square planar with Cl–Pd–N and P–Pd–P bond angles of almost 180°.

Carbons C(1) and C(2) do not lie on the mean plane through atoms Cl, Pd, P(1), P(2), N, Si(1), and Si(2) but are above and below the plane, respectively; however, angles close to tetrahedral values are maintained about both carbon atoms. Deviations, similar to those found in **6**, are observed for the Pd–P(1)–C(25) and Pd–P(2)–C(7) angles. Cl···C(7) and Cl···C(25) intramolecular distances are 3.540 (2) and 3.552 (2) Å, respectively.

We have extended this metathesis reaction utilizing the lithium salt **5** to generate the platinum(II) complex $[PtClN(SiMe_2CH_2PPh_2)_2]$ (**8**) and complete the incorporation of this ligand into the metals of the nickel triad. Thus **8** is produced from the reaction of **5** with Zeise's salt $K[Pt(C_2H_4)Cl_3]$ in THF at 0 °C. Other platinum(II) precursors such as $PtCl_2(COD)$ (COD = 1,5-cyclooctadiene), *trans*-$PtCl_2(PR_3)_2$ (R = Ph or Et), $PtCl_2(PhCN)_2$, and *trans*-$Pt(H)Cl(PEt_3)_2$ only gave intractable mixtures with **8** as a minor component. Presumably **8** is isostructural with the palladium derivative **7** as evidenced by the "virtual" triplet for the methylene resonances in the ^1H NMR (Table I); coupling to platinum-195 (^{195}Pt, 33.7% natural abundance, spin $^1/_2$) further splits this resonance into a 1:4:1 triplet.

The complexes **6**, **7**, and **8** are moisture-sensitive solids which can be handled in dry air for short periods. They are very soluble in cyclohexane and other more polar organic solvents but only slightly soluble in pentane or hexane.

We have also investigated the coordination chemistry of the free ligand **4**. Stirring a THF solution of $NiCl_2$·DME and **4** produces green needles of the formula $[NiCl_2NH(SiMe_2CH_2PPh_2)_2]$ (**9**); recrystallization from CH_2Cl_2/hexane produces dark blue blocks of the same formula. The ^1H NMR of **9** consists of many broadened and shifted peaks indicative of a tetrahedral to square-planar type equilibrium, well-known for a number of nickel(II) bis(phosphine) complexes.[43]

The crystal structure of **9** consists of discrete molecules of $[NiCl_2NH(SiMe_2CH_2PPh_2)_2]$. With the exception of two possible weak C–H···Cl interactions [C(6)–H(6b)···Cl (1) (1 − *x*, 1 − *y*, 1 − *z*) and C(10)–H(10)···Cl(2) (1 − *x*, 1 − *y*, 1 − *z*); H···Cl = 2.85 (5) and 2.88 (3) Å, C–Cl = 3.747 (4) and 3.622 (3) Å, C–H···Cl = 157 (2) and 144 (2)°], all intermolecular distances correspond to normal van der Waals contacts.

(43) For leading references, see: Holm, R. H. In "Dynamic Nuclear Magnetic Resonance Spectroscopy"; Jackman, L. M.; Cotton, F. A., Eds.; Academic Press: New York, 1975; Chapter 9, p 328.

Table V. Final Positional (Fractional, ×10⁵; H, ×10⁴) and Isotropic Thermal Parameters ($U \times 10^3$ Å²) with Estimated Standard Deviations in Parentheses for $[NiCl_2NH(SiMe_2CH_2PPh_2)_2]$, 9

atom	x	y	z	U_{eq}/U_{iso}	atom	x	y	z	U_{eq}/U_{iso}
Ni	52063 (4)	37706 (3)	24406 (2)	34	H(N)	2869 (36)	8311 (36)	1891 (19)	46 (10)
Cl(1)	46633 (10)	32237 (9)	14635 (5)	56	H(1a)	1483 (31)	5550 (30)	2024 (17)	42 (7)
Cl(2)	66435 (9)	23264 (9)	34186 (5)	56	H(1b)	452 (38)	5932 (35)	2772 (19)	53 (9)
P(1)	28619 (7)	46637 (7)	30937 (4)	32	H(2a)	5710 (36)	5963 (37)	538 (19)	53 (10)
P(2)	61336 (7)	54891 (7)	17811 (4)	31	H(2b)	5949 (39)	7096 (38)	607 (20)	65 (10)
Si(1)	8830 (8)	79287 (8)	21673 (4)	35	H(3a)	−1424 (53)	8760 (47)	1829 (25)	93 (15)
Si(2)	33459 (8)	78738 (8)	7614 (4)	37	H(3b)	−429 (55)	8279 (55)	1197 (29)	102 (20)
N	24498 (25)	80793 (25)	16764 (14)	38	H(3c)	−824 (55)	9628 (57)	1293 (30)	105 (18)
C(1)	12773 (30)	59276 (29)	25142 (17)	37	H(4a)	1058 (42)	8569 (40)	3284 (21)	55 (11)
C(2)	53972 (31)	66237 (32)	8361 (16)	39	H(4b)	−98 (43)	9860 (44)	2758 (22)	84 (12)
C(3)	−6639 (43)	87890 (52)	15096 (26)	59	H(4c)	−614 (46)	8661 (43)	3272 (23)	93 (13)
C(4)	2679 (43)	88700 (35)	29898 (21)	52	H(5a)	3685 (38)	9517 (36)	−379 (21)	61 (10)
C(5)	32034 (44)	96630 (38)	1125 (22)	56	H(5b)	3675 (40)	10121 (39)	340 (20)	73 (11)
C(6)	25499 (44)	70848 (49)	2850 (22)	57	H(5c)	2224 (47)	10312 (44)	76 (23)	82 (13)
C(7)	25625 (28)	54449 (26)	39311 (14)	34	H(6a)	1490 (53)	7622 (48)	175 (25)	97 (15)
C(8)	12423 (35)	57669 (33)	44084 (16)	44	H(6b)	3004 (41)	7053 (39)	−239 (23)	73 (11)
C(9)	9727 (39)	64513 (35)	50090 (18)	53	H(6c)	2703 (46)	6194 (48)	585 (25)	96 (14)
C(10)	20010 (39)	68286 (33)	51488 (18)	50	H(8)	559 (38)	5567 (36)	4268 (19)	57 (10)
C(11)	33225 (38)	64981 (34)	46885 (20)	52	H(9)	105 (37)	6656 (35)	5311 (19)	56 (9)
C(12)	36040 (33)	58107 (31)	40773 (18)	44	H(10)	1855 (37)	7225 (37)	5545 (20)	57 (10)
C(13)	25586 (31)	30241 (27)	35377 (16)	42	H(11)	4004 (38)	6716 (36)	4789 (20)	59 (10)
C(14)	31939 (38)	21025 (32)	42395 (22)	59	H(12)	4489 (35)	5648 (33)	3752 (18)	47 (8)
C(15)	29537 (49)	8532 (38)	45809 (29)	80	H(14)	3848 (37)	2365 (35)	4466 (19)	58 (9)
C(16)	21145 (59)	5328 (42)	42306 (32)	91	H(15)	3342 (39)	323 (41)	5065 (22)	67 (11)
C(17)	14994 (59)	14246 (47)	35418 (28)	83	H(16)	1955 (48)	−252 (48)	4517 (24)	94 (14)
C(18)	17326 (46)	26666 (38)	31898 (21)	61	H(17)	940 (50)	1162 (49)	3256 (26)	102 (15)
C(19)	61275 (28)	67227 (27)	23183 (15)	35	H(18)	1409 (45)	3188 (45)	2684 (25)	87 (13)
C(20)	54746 (34)	82492 (31)	20581 (19)	46	H(20)	4982 (33)	8707 (32)	1545 (19)	48 (8)
C(21)	54906 (41)	91254 (38)	25023 (25)	64	H(21)	5085 (41)	10138 (42)	2258 (22)	80 (12)
C(22)	61637 (44)	84823 (44)	32033 (24)	65	H(22)	6228 (47)	9084 (47)	3419 (25)	97 (15)
C(23)	68267 (43)	69940 (43)	34556 (21)	61	H(23)	7288 (39)	6582 (39)	3917 (22)	67 (11)
C(24)	68113 (35)	60976 (34)	30240 (18)	47	H(24)	7228 (39)	5073 (40)	3190 (20)	71 (11)
C(25)	81133 (27)	45100 (27)	15080 (14)	34	H(26)	8558 (39)	6236 (39)	1163 (20)	69 (11)
C(26)	89781 (34)	52645 (34)	12007 (20)	50	H(27)	10959 (38)	5043 (36)	830 (19)	57 (10)
C(27)	104513 (36)	45442 (42)	9713 (22)	57	H(28)	12178 (39)	2571 (36)	846 (19)	61 (9)
C(28)	111146 (35)	30560 (39)	10364 (20)	58	H(29)	10693 (50)	1334 (50)	1344 (26)	108 (15)
C(28)	102800 (39)	22967 (38)	13291 (23)	66	H(30)	8141 (40)	2541 (38)	1737 (20)	59 (10)
C(30)	87849 (34)	30074 (32)	15609 (20)	52					

Table XII. Bond Lengths (Å) with Estimated Standard Deviations in Parentheses for $[NiClN(SiMe_2CH_2PPh_2)_2]$, 6

bond	uncorr	corr	bond	uncorr	corr
Ni-Cl	2.1703 (6)	2.172	C(9)-C(10)	1.368 (4)	1.374
Ni-P(1)	2.2086 (6)	2.212	C(10)-C(11)	1.363 (4)	1.371
Ni-P(2)	2.1975 (5)	2.201	C(11)-C(12)	1.387 (3)	1.391
Ni-N	1.924 (2)	1.929	C(13)-C(14)	1.371 (3)	1.384
P(1)-C(1)	1.816 (2)	1.819	C(13)-C(18)	1.384 (3)	1.395
P(1)-C(7)	1.825 (2)	1.830	C(14)-C(15)	1.381 (4)	1.384
P(1)-C(13)	1.817 (2)	1.822	C(15)-C(16)	1.357 (4)	1.367
P(2)-C(2)	1.807 (2)	1.810	C(16)-C(17)	1.357 (4)	1.371
P(2)-C(19)	1.824 (2)	1.828	C(17)-C(18)	1.384 (4)	1.387
P(2)-C(25)	1.813 (2)	1.818	C(19)-C(20)	1.389 (3)	1.394
Si(1)-N	1.710 (2)	1.716	C(19)-C(24)	1.381 (3)	1.390
Si(1)-C(1)	1.887 (2)	1.895	C(20)-C(21)	1.381 (4)	1.383
Si(1)-C(3)	1.859 (3)	1.868	C(21)-C(22)	1.374 (4)	1.383
Si(1)-C(4)	1.867 (3)	1.876	C(22)-C(23)	1.368 (4)	1.373
Si(2)-N	1.713 (2)	1.721	C(23)-C(24)	1.390 (4)	1.392
Si(2)-C(2)	1.893 (3)	1.904	C(25)-C(26)	1.371 (3)	1.381
Si(2)-C(5)	1.857 (4)	1.867	C(25)-C(30)	1.381 (3)	1.395
Si(2)-C(6)	1.860 (4)	1.872	C(26)-C(27)	1.381 (4)	1.384
C(7)-C(8)	1.381 (3)	1.389	C(27)-C(28)	1.364 (4)	1.379
C(7)-C(12)	1.387 (3)	1.394	C(28)-C(29)	1.349 (4)	1.356
C(8)-C(9)	1.386 (4)	1.390	C(29)-C(30)	1.385 (4)	1.389

Unlike molecules of **6** and **7** which both have approximate twofold symmetry, molecules of **9** (Figure 5) display no elements of symmetry in the solid state. The coordination geometry about the nickel atom is distorted tetrahedral with bond angles at Ni ranging from 98.89 (3)° for Cl(1)–Ni–P(1) to 130.36 (3)° for Cl–Ni–Cl (Table XVII). The irregularity of the Ni coordination sphere is reflected by the small but significant differences between chemically equivalent Ni–Cl (2.2216 (8) and 2.2058 (8) Å) and Ni–P (2.3180 (7) and 2.3469 (7) Å) bonds. This structure is very similar to that of the closely related molecule $[NiCl_2O(CH_2CH_2PPh_2)_2]$[44] which has Ni–Cl = 2.229 (5) and 2.210 (4) Å and Ni–P = 2.309 (4) and 2.321 (3) Å. Except for the P–Ni–P angle (107.1 (1)° vs. 116.99 (2)° in **9**), bond angles about the nickel atom in **9** deviate in the same sense,

(44) Greene, P. T.; Sacconi, L. *J. Chem. Soc. A.* **1970**, 866.

Table XIII. Bond Lengths (Å) with Estimated Standard Deviations in Parentheses for $[PdClN(SiMe_2CH_2PPh_2)_2]\cdot CH_3C_6H_5$, 7

bond	uncorr	corr	bond	uncorr	corr
Pd-P(1)	2.3078 (5)	2.311	C(13)-C(18)	1.372 (3)	1.388
Pd-P(2)	2.3112 (5)	2.314	C(14)-C(15)	1.384 (4)	1.389
Pd-Cl	2.3143 (6)	2.317	C(15)-C(16)	1.355 (6)	1.372
Pd-N	2.063 (2)	2.069	C(16)-C(17)	1.359 (5)	1.370
P(1)-C(1)	1.805 (2)	1.809	C(17)-C(18)	1.380 (4)	1.384
P(1)-C(7)	1.821 (2)	1.827	C(19)-C(20)	1.392 (3)	1.402
P(1)-C(13)	1.819 (2)	1.823	C(19)-C(24)	1.376 (4)	1.388
P(2)-C(2)	1.807 (2)	1.811	C(20)-C(21)	1.390 (4)	1.395
P(2)-C(19)	1.816 (2)	1.821	C(21)-C(22)	1.354 (5)	1.366
P(2)-C(25)	1.820 (2)	1.825	C(22)-C(23)	1.373 (5)	1.382
Si(1)-N	1.713 (2)	1.719	C(23)-C(24)	1.383 (4)	1.388
Si(1)-C(1)	1.885 (3)	1.891	C(25)-C(26)	1.380 (3)	1.394
Si(1)-C(3)	1.873 (3)	1.881	C(25)-C(30)	1.379 (4)	1.391
Si(1)-C(4)	1.871 (4)	1.879	C(26)-C(27)	1.385 (4)	1.388
Si(2)-N	1.711 (2)	1.717	C(27)-C(28)	1.361 (5)	1.372
Si(2)-C(2)	1.885 (3)	1.892	C(28)-C(29)	1.361 (5)	1.376
Si(2)-C(5)	1.872 (3)	1.881	C(29)-C(30)	1.385 (4)	1.389
Si(2)-C(6)	1.855 (3)	1.863	C(31)-C(32)	1.396 (6)	1.413
C(7)-C(8)	1.374 (4)	1.390	C(31)-C(36)	1.367 (5)	1.386
C(7)-C(12)	1.370 (4)	1.383	C(31)-C(37)	1.492 (7)	1.503
C(8)-C(9)	1.388 (4)	1.394	C(32)-C(33)	1.359 (8)	1.374
C(9)-C(10)	1.345 (6)	1.357	C(33)-C(34)	1.383 (8)	1.400
C(10)-C(11)	1.360 (6)	1.376	C(34)-C(35)	1.352 (7)	1.367
C(11)-C(12)	1.386 (4)	1.391	C(35)-C(36)	1.365 (6)	1.379
C(13)-C(14)	1.388 (4)	1.399			

Table XIV. Bond Lengths (Å) with Estimated Standard Deviations in Parentheses for $[NiCl_2NH(SiMe_2CH_2PPh_2)_2]$, 9

bond	uncorr	corr	bond	uncorr	corr
Ni-Cl(1)	2.2216 (8)	2.2251	C(9)-C(10)	1.373 (5)	1.379
Ni-Cl(2)	2.2058 (8)	2.2081	C(10)-C(11)	1.377 (5)	1.383
Ni-P(1)	2.3180 (7)	2.3202	C(11)-C(12)	1.390 (4)	1.392
Ni-P(2)	2.3469 (7)	2.3502	C(13)-C(14)	1.394 (5)	1.403
P(1)-C(1)	1.815 (3)	1.817	C(13)-C(18)	1.373 (5)	1.382
P(1)-C(7)	1.814 (3)	1.817	C(14)-C(15)	1.397 (5)	1.402
P(1)-C(13)	1.826 (3)	1.832	C(15)-C(16)	1.360 (7)	1.370
P(2)-C(2)	1.817 (3)	1.820	C(16)-C(17)	1.363 (7)	1.371
P(2)-C(19)	1.826 (3)	1.831	C(17)-C(18)	1.389 (4)	1.393
P(2)-C(25)	1.824 (3)	1.829	C(19)-C(20)	1.392 (4)	1.400
Si(1)-N	1.718 (2)	1.724	C(19)-C(24)	1.389 (4)	1.396
Si(1)-C(1)	1.885 (3)	1.891	C(20)-C(21)	1.389 (5)	1.393
Si(1)-C(3)	1.859 (4)	1.866	C(21)-C(22)	1.376 (6)	1.382
Si(1)-C(4)	1.848 (3)	1.854	C(22)-C(23)	1.357 (5)	1.365
Si(2)-N	1.718 (2)	1.723	C(23)-C(24)	1.390 (4)	1.394
Si(2)-C(2)	1.886 (3)	1.892	C(25)-C(26)	1.390 (4)	1.398
Si(2)-C(5)	1.861 (3)	1.868	C(25)-C(30)	1.384 (4)	1.395
Si(2)-C(6)	1.845 (3)	1.851	C(26)-C(27)	1.367 (4)	1.370
C(7)-C(8)	1.390 (4)	1.397	C(27)-C(28)	1.367 (5)	1.379
C(7)-C(12)	1.382 (4)	1.388	C(28)-C(29)	1.366 (5)	1.373
C(8)-C(9)	1.373 (4)	1.376	C(29)-C(30)	1.384 (4)	1.387

Table XV. Bond Angles (Deg) with Estimated Standard Deviations in Parentheses for $[NiClN(SiMe_2CH_2PPh_2)_2]$, 6

Cl-Ni-P(1)	95.40 (2)	C(3)-Si(1)-C(4)	107.2 (2)	C(14)-C(13)-C(18)	118.2 (2)
Cl-Ni-P(2)	93.74 (2)	N-Si(2)-C(2)	105.15 (9)	C(13)-C(14)-C(15)	120.3 (2)
Cl-Ni-N	178.16 (6)	N-Si(2)-C(5)	113.8 (2)	C(14)-C(15)-C(16)	121.0 (3)
P(1)-Ni-P(2)	167.72 (2)	N-Si(2)-C(6)	112.7 (2)	C(15)-C(16)-C(17)	119.7 (3)
P(1)-Ni-N	85.96 (6)	C(2)-Si(2)-C(5)	108.6 (2)	C(16)-C(17)-C(18)	120.0 (3)
P(2)-Ni-N	85.10 (5)	C(2)-Si(2)-C(6)	107.4 (2)	C(13)-C(18)-C(17)	120.9 (3)
Ni-P(1)-C(1)	102.96 (9)	C(5)-Si(2)-C(6)	108.8 (3)	P(2)-C(19)-C(20)	119.3 (2)
Ni-P(1)-C(7)	120.11 (7)	Ni-N-Si(1)	118.02 (9)	P(2)-C(19)-C(24)	122.1 (2)
Ni-P(1)-C(13)	115.14 (7)	Ni-N-Si(2)	113.83 (10)	C(20)-C(19)-C(24)	118.5 (2)
C(1)-P(1)-C(7)	105.73 (10)	Si(1)-N-Si(2)	128.13 (10)	C(19)-C(20)-C(21)	121.0 (2)
C(1)-P(1)-C(13)	107.27 (11)	P(1)-C(1)-Si(1)	105.70 (12)	C(20)-C(21)-C(22)	119.9 (2)
C(7)-P(1)-C(13)	104.67 (10)	P(2)-C(2)-Si(2)	104.36 (12)	C(21)-C(22)-C(23)	119.9 (3)
Ni-P(2)-C(2)	106.98 (8)	P(1)-C(7)-C(8)	124.1 (2)	C(22)-C(23)-C(24)	120.5 (3)
Ni-P(2)-C(19)	121.29 (7)	P(1)-C(7)-C(12)	116.8 (2)	C(19)-C(24)-C(23)	120.2 (2)
Ni-P(2)-C(25)	106.46 (7)	C(8)-C(7)-C(12)	119.1 (2)	P(2)-C(25)-C(26)	118.1 (2)
C(2)-P(2)-C(19)	108.49 (11)	C(7)-C(8)-C(9)	120.1 (3)	P(2)-C(25)-C(30)	123.5 (2)
C(2)-P(2)-C(25)	108.56 (11)	C(8)-C(9)-C(10)	120.2 (3)	C(26)-C(25)-C(30)	118.4 (2)
C(19)-P(2)-C(25)	104.54 (9)	C(9)-C(10)-C(11)	120.3 (3)	C(25)-C(26)-C(27)	121.2 (3)
N-Si(1)-C(1)	104.15 (9)	C(10)-C(11)-C(12)	120.2 (3)	C(26)-C(27)-C(28)	119.6 (3)
N-Si(1)-C(3)	114.6 (2)	C(7)-C(12)-C(11)	120.1 (2)	C(27)-C(28)-C(29)	120.0 (3)
N-Si(1)-C(4)	114.87 (15)	P(1)-C(13)-C(14)	118.8 (2)	C(28)-C(29)-C(30)	121.0 (3)
C(1)-Si(1)-C(3)	107.4 (2)	P(1)-C(13)-C(18)	123.0 (2)	C(25)-C(30)-C(29)	119.7 (3)
C(1)-Si(1)-C(4)	108.3 (2)				

Table XVI. Bond Angles (Deg) with Estimated Standard Deviations in Parentheses for $[PdClN(SiMe_2CH_2PPh_2)_2]\cdot CH_3C_6H_5$, 7

P(1)-Pd-P(2)	177.11 (2)	N-Si(2)-C(5)	112.90 (15)	C(13)-C(18)-C(17)	120.3 (3)
P(1)-Pd-Cl	90.56 (2)	N-Si(2)-C(6)	113.36 (14)	P(2)-C(19)-C(20)	121.5 (2)
P(1)-Pd-N	88.66 (5)	C(2)-Si(2)-C(5)	105.9 (2)	P(2)-C(19)-C(24)	119.0 (2)
P(2)-Pd-Cl	91.29 (2)	C(2)-Si(2)-C(6)	109.8 (2)	C(20)-C(19)-C(24)	119.4 (2)
P(2)-Pd-N	89.47 (5)	C(5)-Si(2)-C(6)	108.9 (2)	C(19)-C(20)-C(21)	119.4 (3)
Cl-Pd-N	179.04 (5)	Pd-N-Si(1)	119.34 (10)	C(20)-C(21)-C(22)	120.7 (3)
Pd-P(1)-C(1)	106.77 (8)	Pd-N-Si(2)	118.39 (9)	C(21)-C(22)-C(23)	120.1 (3)
Pd-P(1)-C(7)	120.39 (7)	Si(1)-N-Si(2)	122.27 (11)	C(22)-C(23)-C(24)	120.2 (4)
Pd-P(1)-C(13)	111.94 (7)	P(1)-C(1)-Si(1)	106.90 (12)	C(19)-C(24)-C(23)	120.1 (3)
C(1)-P(1)-C(7)	108.28 (11)	P(2)-C(2)-Si(2)	107.22 (12)	P(2)-C(25)-C(26)	123.2 (2)
C(1)-P(1)-C(13)	104.93 (11)	P(1)-C(7)-C(8)	121.1 (2)	P(2)-C(25)-C(30)	118.6 (2)
C(7)-P(1)-C(13)	103.52 (11)	P(1)-C(7)-C(12)	120.6 (2)	C(26)-C(25)-C(30)	118.2 (2)
Pd-P(2)-C(2)	105.88 (8)	C(8)-C(7)-C(12)	118.2 (3)	C(25)-C(26)-C(27)	120.1 (3)
Pd-P(2)-C(19)	115.27 (8)	C(7)-C(8)-C(9)	119.9 (3)	C(26)-C(27)-C(28)	121.1 (3)
Pd-P(2)-C(25)	116.38 (7)	C(8)-C(9)-C(10)	121.0 (4)	C(27)-C(28)-C(29)	119.4 (3)
C(2)-P(2)-C(19)	107.97 (12)	C(9)-C(10)-C(11)	120.1 (3)	C(28)-C(29)-C(30)	120.2 (3)
C(2)-P(2)-C(25)	107.03 (11)	C(10)-C(11)-C(12)	119.4 (4)	C(25)-C(30)-C(29)	121.0 (3)
C(19)-P(2)-C(25)	103.85 (10)	C(7)-C(12)-C(11)	121.3 (3)	C(32)-C(31)-C(36)	117.3 (4)
N-Si(1)-C(1)	105.61 (10)	P(1)-C(13)-C(14)	120.6 (2)	C(32)-C(31)-C(37)	120.7 (4)
N-Si(1)-C(3)	113.59 (15)	P(1)-C(13)-C(18)	121.0 (2)	C(36)-C(31)-C(37)	122.0 (4)
N-Si(1)-C(4)	113.7 (2)	C(14)-C(13)-C(18)	118.4 (2)	C(31)-C(32)-C(33)	120.2 (5)
C(1)-Si(1)-C(3)	109.2 (2)	C(13)-C(14)-C(15)	120.3 (3)	C(32)-C(33)-C(34)	121.1 (5)
C(1)-Si(1)-C(4)	106.1 (2)	C(14)-C(15)-C(16)	120.4 (3)	C(33)-C(34)-C(35)	119.0 (6)
C(3)-Si(1)-C(4)	108.3 (2)	C(15)-C(16)-C(17)	119.7 (3)	C(34)-C(35)-C(36)	120.1 (6)
N-Si(2)-C(2)	105.66 (10)	C(16)-C(17)-C(18)	120.9 (3)	C(31)-C(36)-C(35)	122.4 (4)

Table XVII. Bond Angles (Deg) with Estimated Standard Deviations in Parentheses for $[NiCl_2NH(SiMe_2CH_2PPh_2)_2]$, 9

Cl(1)-Ni-Cl(2)	130.36 (3)	C(1)-Si(1)-C(4)	112.42 (14)	C(13)-C(14)-C(15)	119.4 (4)
Cl(1)-Ni-P(1)	98.89 (3)	C(3)-Si(1)-C(4)	108.5 (2)	C(14)-C(15)-C(16)	120.4 (4)
Cl(1)-Ni-P(2)	103.33 (3)	N-Si(2)-C(2)	111.12 (12)	C(15)-C(16)-C(17)	120.4 (4)
Cl(2)-Ni-P(1)	102.40 (3)	N-Si(2)-C(5)	111.5 (2)	C(16)-C(17)-C(18)	120.1 (4)
Cl(2)-Ni-P(2)	105.81 (3)	N-Si(2)-C(6)	110.24 (15)	C(13)-C(18)-C(17)	120.5 (4)
P(1)-Ni-P(2)	116.99 (2)	C(2)-Si(2)-C(5)	106.01 (15)	P(2)-C(19)-C(20)	123.5 (2)
Ni-P(1)-C(1)	118.46 (10)	C(2)-Si(2)-C(6)	108.7 (2)	P(2)-C(19)-C(24)	118.0 (2)
Ni-P(1)-C(7)	119.59 (9)	C(5)-Si(2)-C(6)	109.2 (2)	C(20)-C(19)-C(24)	118.6 (3)
Ni-P(1)-C(13)	103.94 (8)	Si(1)-N-Si(2)	134.1 (2)	C(19)-C(20)-C(21)	120.5 (3)
C(1)-P(1)-C(7)	104.85 (12)	P(1)-C(1)-Si(1)	118.85 (14)	C(20)-C(21)-C(22)	119.9 (3)
C(1)-P(1)-C(13)	105.05 (13)	P(2)-C(2)-Si(2)	120.94 (15)	C(21)-C(22)-C(23)	120.1 (3)
C(7)-P(1)-C(13)	102.92 (12)	P(1)-C(7)-C(8)	120.5 (2)	C(22)-C(23)-C(24)	120.9 (4)
Ni-P(2)-C(2)	116.15 (10)	P(1)-C(7)-C(12)	120.5 (2)	C(19)-C(24)-C(23)	120.0 (3)
Ni-P(2)-C(19)	118.86 (8)	C(8)-C(7)-C(12)	118.9 (3)	P(2)-C(25)-C(26)	120.9 (2)
Ni-P(2)-C(25)	109.17 (8)	C(7)-C(8)-C(9)	120.5 (3)	P(2)-C(25)-C(30)	121.2 (2)
C(2)-P(2)-C(19)	106.59 (13)	C(8)-C(9)-C(10)	120.6 (3)	C(26)-C(25)-C(30)	117.9 (2)
C(2)-P(2)-C(25)	102.34 (12)	C(9)-C(10)-C(11)	119.6 (3)	C(25)-C(26)-C(27)	121.2 (3)
C(19)-P(2)-C(25)	101.53 (11)	C(10)-C(11)-C(12)	120.3 (3)	C(26)-C(27)-C(28)	120.7 (3)
N-Si(1)-C(1)	109.87 (12)	C(7)-C(12)-C(11)	120.2 (3)	C(27)-C(28)-C(29)	119.0 (3)
N-Si(1)-C(3)	111.8 (2)	P(1)-C(13)-C(14)	119.4 (2)	C(28)-C(29)-C(30)	121.2 (3)
N-Si(1)-C(4)	108.8 (2)	P(1)-C(13)-C(18)	121.4 (2)	C(25)-C(30)-C(29)	120.1 (3)
C(1)-Si(1)-C(3)	105.5 (2)	C(14)-C(13)-C(18)	119.1 (3)		

Table XVIII. Intraannular Torsion Angles for the Chelate Rings in 6, 7, and 9 with Estimated Standard Deviations in Parentheses

atoms	6, M = Ni	7, M = Pd
N-M-P(1)-C(1)	43.77 (10)	−18.87 (11)
M-P(1)-C(1)-Si(1)	−37.84 (13)	34.17 (14)
P(1)-C(1)-Si(1)-N	13.30 (15)	−36.41 (15)
C(1)-Si(1)-N-M	23.14 (14)	23.61 (15)
Si(1)-N-M-P(1)	−40.79 (10)	−3.47 (11)
N-M-P(2)-C(2)	40.96 (11)	−17.91 (11)
M-P(2)-C(2)-Si(2)	−24.92 (14)	34.13 (14)
P(2)-C(2)-Si(2)-N	−4.95 (15)	−38.0 (2)
C(2)-Si(2)-N-M	39.83 (14)	25.63 (15)
Si(2)-N-M-P(2)	−47.86 (9)	−5.20 (11)

atoms	9
P(2)-Ni-P(1)-C(1)	64.99 (10)
Ni-P(1)-C(1)-Si(1)	−80.2 (2)
P(1)-C(1)-Si(1)-N	53.0 (2)
C(1)-Si(1)-N-Si(2)	74.4 (2)
Si(1)-N-Si(2)-C(2)	−130.1 (2)
N-Si(2)-C(2)-P(2)	13.7 (2)
Si(2)-C(2)-P(2)-Ni	60.2 (2)
C(2)-P(2)-Ni-P(1)	−77.74 (11)

but to a greater degree, from the idealized tetrahedral value than do those in $[NiCl_2O(CH_2CH_2PPh_2)_2]$. The large difference between the P–Ni–P angles in the two compounds probably results from the steric requirements of the respective ligands, in particular the replacement of two CH_2 groups by $SiMe_2$ moieties. The Ni–Cl and Ni–P distances lie within the ranges normally observed for tetrahedral Ni(II) but are considerably longer than the corresponding bonds in the square-planar complex **6**.

The N–H portion of the ligand backbone of **9** does not interact with the metal center (Ni···H = 4.13 (4), Ni···N = 4.044 (2) Å) nor is the N–H group involved in any hydrogen bonding, being sterically blocked as is evident in Figure 5. These data are consistent with the observed N–H stretching frequency of 3365 cm^{-1} (KBr) which is identical with that found for the free ligand. This is in sharp contrast with that found for the closely related molecule, $[NiBr_2NH(CH_2CH_2PPh_2)_2]$,[45] wherein the nitrogen atom is coordinated to the metal in the solid state. The resulting five-coordinate structure is square pyramidal with a bromine in the apical position (mirror symmetry, Ni–N = 2.01 (3), Ni–P = 2.172 (5), N–Br(basal) = 2.333 (7), and Ni–Br(apical) = 2.698 (7) Å). Although steric arguments can be invoked, the lack of coordination of the N–H group in

(45) Orioli, P. L.; Sacconi, L. *Chem. Commun.* **1968**, 1310.

9 is best accounted for by delocalization[46] of the nitrogen lone pair into low-lying silicon d orbitals, thus making it unavailable for donation to a metal. The unusual eight-membered chelate ring of **9** which results has a conformation which is best characterized (on the basis of the intraannular torsion angles) as a distorted twist-boat–chair.[47] There are several intramolecular steric interactions of importance which include van der Waals contacts of the types: methyl–methyl (C(3)···C(6) = 3.553 (6) Å), methyl–phenyl (C(4)···C(7) = 3.382 (4) Å), phenyl–phenyl (C(12)···C(24) = 3.534 (4) and H(12)···C(24) = 2.65 (3) Å), and NH–phenyl (H(N)···H(20) = 2.32 (4) Å).

The phenyl rings in **6**, **7**, and **9** are, in general, slightly but significantly nonplanar (maximum deviation from C_6 plane 0.01 Å) with the phosphorus atoms significantly displaced from the phenyl mean planes (by up to 0.13 Å). The averaged corrected bond lengths and bond angles for the PC_6H_5 groups are in excellent agreement with tabulated values.[48] It is interesting to note that in spite of the considerable differences between corresponding bond angles (a result of both ring-size and steric effects), the bond lengths in the chelating ligands in **6** and **7** differ very little fromthose in **9**. The Si–N, Si–CH_3, and P–C(phenyl) distances (averaged for all three compounds) of 1.714 (3), 1.861 (9), 1.821 (4) Å, respectively, are as expected. An interesting feature common to all three structures is the geometry at the methylene carbon atoms C(1) and C(2) where the bonds to silicon (mean Si–CH_2 = 1.887 (3) Å) are longer than the Si–CH_3 bonds by an average of 0.026 Å (all individual differences being statistically significant), and the bonds to phosphorus (mean P–CH_2 = 1.811 (5) Å) are shorter than the P–C (phenyl) bonds by an average of 0.010 Å. In the case of the P–C bonds this is the opposite of what would be expected on the basis of σ-hybridization effects and mildly suggests an alternation of bond strengths in the N–Si–C–P–M fragments.

The analogous reaction of the free ligand **4** with both $PdCl_2(PhCN)_2$ and $K[Pt(C_2H_4)Cl_3]$ produces, respectively, $[PdCl_2NH(SiMe_2CH_2PPh_2)_2]$, **10**, and $[PtCl_2NH(SiMe_2CH_2PPh_2)_2]$, **11**, as diamagnetic, poorly soluble solids. We formulate **10** and **11** as square-planar com-

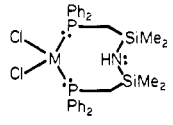

plexes with cis disposed phosphines on the basis of their ^1H NMR spectra wherein the methylene protons appear as broadened resonances indicative of weakly coupled phosphorus nuclei due to their cis orientation on the metal. Interestingly the N–H stretching frequency decreases to 3305 cm^{-1} for the palladium complex **10** and further to 3280 cm^{-1} for the platinum derivative **11** as compared to the free ligand (ν_{NH} = 3365 cm^{-1}). The low solubility of **10** and **11** has precluded extensive solution studies to trace this decrease in ν_{NH}.

Probably the most useful reaction of the bidentate amine dichlorides **9**, **10**, and **11** is their facile conversion into the corresponding tridentate amido derivatives **6**, **7**, and **8** with base. Optimum results have been obtained with NEt_3; pyridine and 2,4,6-trimethylpyridine are not effective in this conversion as only starting materials are isolated with **10** and **11**. With pyridine, displacement of the phosphines

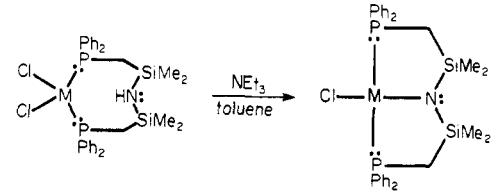

9,10,11 **6,7,8**

of **9** occurs to produce $NiCl_2(py)_4$ (py = pyridine). Coordination via the phosphine donors is a crucial factor in this reaction with NEt_3, as is the relative insolubility of NEt_3·HCl in toluene. However, since the reaction of free $HN(SiMe_3)_2$ with $NiCl_2(PR_3)_2$ (R = Me or Ph) and NEt_3 produces no nickel amide species (only starting materials are isolated), it would seem that coordination followed by activation of the distal N–H bond is the determining feature. Although it is tempting to suggest a transient oxidative addition step for this formation, no such intermediate has been detected even for the platinum derivative.

Formation of Metal–Carbon Bonds. The incorporation of simple alkyl groups into transition-metal complexes continues to be the object of much research, notably because the subsequent stability and reactivity of the so formed transition metal–carbon bond can sometimes be related to its potential for use in organic synthesis and homogeneous catalysis.[49] We have investigated the reaction of Grignard reagents with the tridentate amido phosphine complexes and have found that the nickel and palladium chloro derivatives, **6** and **7**, respectively, readily undergo metathesis with simple Grignards, RMgX (R = CH_3, $CH_2CH{=}CH_2$, $CH{=}CH_2$, and C_6H_5), in toluene/ether mixtures to generate the corresponding carbon-bonded ligands. The use of alkyllithium reagents (i.e.,

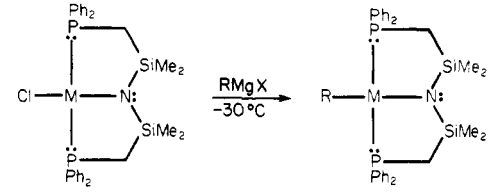

6,7

MeLi or PhLi) does produce the corresponding carbon-bonded complexes, but the yields are invariably lower than via the Grignard route. The only constraints in the choice of R in RMgX is that there be no β-hydrogen atoms, thus avoiding β-elimination sequences. Table I lists these derivatives and their ^1H NMR patterns. When R is allyl (C_3H_5), two limiting bonding modes are observed, depending on the metal; thus the ^1H NMR of the complex $[Ni(C_3H_5)N(SiMe_2CH_2PPh_2)_2]$ shows a classic AX_4 pattern for the allyl protons (with phosphorus decoupled) which indicates equivalent syn and anti protons via rapid η^3–η^1 interconversions on the NMR time scale. Even at −80 °C, the AX_4 pattern persists. For the analogous palladium complex $[Pd(C_3H_5)N(SiMe_2CH_2PPh_2)_2]$ on the other hand, we observe only the η^1 mode of bonding in the ^1H NMR at ambient temperatures. As the temperature is raised, the resonances of the allyl ligand broaden and above 50 °C, rapid η^3–η^1 interconversions occur as evidenced by the appearance of the AX_4 pattern (^{31}P decoupled). All of these complexes can be recrystallized from hexane at low

(46) Reference 3, p 378. Noodleman, L.; Paddock, N. L. *Inorg. Chem.* **1979**, *18*, 354.
(47) Hendrickson, J. B. *J. Am. Chem. Soc.* **1967**, *89*, 7036.
(48) Domenicano, A.; Vaciago, A.; Coulson, C. A. *Acta Crystallogr., Sect. B* **1975**, *B31*, 221.
(49) Collman, J. P.; Hegedus, L. S. "Principles and Applications of Organotransition Metal Chemistry"; University Science Books: Mill Valley, CA, 1980; p 72.
(50) Reference 49, p 213.

temperatures (−30 °C) in the absence of air; at ambient temperatures or higher in solution, some decomposition is observed (darkening of solutions) over a period of hours, but this can be suppressed to some extent by dilution. The isolated crystalline solids are stable at room temperature under N_2.

Unfortunately, we have been unable to form any of the corresponding platinum–carbon bonded species using similar techniques. The action of MeMgCl on **8** in a number of solvent mixtures and at a variety of temperatures was invesigated, but only starting material or intractable mixtures were produced. The use of alkyllithium reagents merely resulted in decomposition products. The anomalous behavior of the platinum chloride bond of **8** is exemplified by the fact that the reaction with standard halide abstraction reagents such as $AgBF_4$ and $AgClO_4$ in CH_2Cl_2 or CH_3CN results in the formation of a silver mirror and no AgCl; no identifiable products have been isolated from these reactions.

Discussion

The results of this study demonstrate that a ligand which contains both the hard donor amido ligand and soft phosphine donors in a chelating array can readily bind to the metals of the nickel triad. While phosphine complexes of nickel, palladium, and platinum are legion, corresponding amide derivatives are extremely rare; indeed, palladium amide complexes were unknown until our efforts in this area. It would appear that our strategy to use the chelate effect is crucial for the synthesis of these derivatives, since prototype reactions in which monodentate amide precursors are utilized generate completely different, if any, products. Thus in the reaction of the lithium salt **5** with soluble nickel(II) precursors, it is reasonable to suggest that coordination by one or both of the phosphine arms occurs *first* followed by metathesis of the chloride to generate the nickel(II)–amide bond. This ensures that, if an electron-transfer process occurs before metathesis, the coordinated end or ends of the ligand serve to cage the incipient radicals to produce no net reduction of the metal. Electron transfer must be important to some extent in the formation of metal amide bonds in order to explain the isolation of nickel(I) amides[38] from nickel(II) starting materials and the complete lack of palladium amides.[12]

Another feature of this work which can be rationalized by prior coordination of the phosphine arms is the facile conversion of the amine dichlorides **9**, **10**, and **11** (where the amine portion is considered to be uncoordinated) to the amide derivatives **6**, **7**, and **8**, in the presence of NEt_3. The reaction can be considered as a modification of the well-known *cyclometalation* reaction[26] except that in our system a distal N–H bond rather than a C–H bond is activated. The mild conditions and overall high yields of this process suggest that it will be a useful method for the incorporation of these hybrid ligands into other transition metals.

The *hard–soft*, hybrid nature of this ligand system deserves some comment. The overall reactivity of these complexes mimics that of straightforward phosphine complexes of the nickel triad; for instance, metathesis by Grignard reagents to generate nickel(II) and palladium(II) carbon bonds proceeds smoothly with no real effect attributable to the metal amide bond other than to anchor the tridentate mode of ligation. However, in the platinum amide complex metathesis of the chloride ligand does not proceed under any conditions that we have investigated; that the chloride bond is trans to the platinum amide bond may be the determining feature, suggesting a strengthening effect of a ligand trans to an amide. As gauged by the Pt–Cl stretching frequency (317 cm^{-1}), the amide ligand exerts a *weak* trans influence,[51] consistent with observed lack of reactivity of the trans Pt–Cl bond.

With the ready availability of nickel(II) and palladium(II) complexes containing both formally uninegative metal nitrogen and metal carbon bonds, we are now in a position to investigate their relative migratory aptitudes with small molecules such as CO and CO_2. This work and related chemistry with other group 8 metals will be reported in due course.

Acknowledgment. We thank Mr. P. Borda for Microanalytical Services and Dr. S. O. Chan and his staff for some of the NMR experiments. Financial support for this research was generously provided by the Department of Chemistry, the Natural, Applied and Health Sciences Fund (UBC), and the Natural Sciences and Engineering Research Council of Canada. Computing funds were provided for by Xerox Corp. and the UBC Computing Centre. P.A.M. thanks the Walter C. Sumner Foundation for a Memorial Fellowship.

Registry No. **3**, 14579-91-0; **4**, 77617-70-0; **5**, 77617-69-7; **6**, 77593-59-0; **7**, 81603-02-3; **8**, 81603-03-4; **9**, 81603-04-5; **10**, 81603-05-6; **11**, 81603-06-7; $[Ni(PMe_3)_2Cl_2]$, 19232-05-4; $[PdClN(SiMe_2CH_2PPh_2)_2]$, 77593-60-3; $(C_6H_5CN)_2PdCl_2$, 14220-64-5; $K[PtCl_3(C_2H_4)]$, 12012-50-9; $Pt(COD)Cl_2$, 12080-32-9; $[Ni(CH_3)N(SiMe_2CH_2PPh_2)_2]$, 81603-07-8; $[Ni(CH_2CH{=}CH_2)N(SiMe_2CH_2PPh_2)_2]$, 81603-08-9; $[Ni(CH{=}CH_2)N(SiMe_2CH_2PPh_2)_2]$, 81610-99-3; $[Ni(C_6H_5)N(SiMe_2CH_2PPh_2)_2]$, 81603-09-0; $[Ni(CN)N(SiMe_2CH_2PPh_2)_2]$, 81603-10-3; $[Pd(CH_3)N(SiMe_2CH_2PPh_2)_2]$, 81603-11-4; $[Pd(CH_2CH{=}CH_2)N(SiMe_2CH_2PPh_2)_2]$, 81603-12-5.

Supplementary Material Available: Anisotropic thermal parameters (Tables VI–VIII), structure factor amplitudes (Tables IX–XI), and bond lengths and angles involving hydrogen atoms and complete lists of torsion angles (Tables XIX–XXVII) (127 pages). Ordering information is given on any current masthead page.

(51) Appleton, T. G.; Clark, H. C.; Manzer, L. E. *Coord. Chem. Rev.* **1973**, *10*, 335.